Extreme mitochondrial DNA divergence underlies genetic conflict over sex determination

Patrice David, Cyril Degletagne, Nathanaelle Saclier, Aurel Jennan, Philippe Jarne, Sandrine Plénet, Lara Konecny, Clémentine François, Laurent Guéguen, Noéline Garcia, et al.

Extreme mitochondrial DNA divergence underlies genetic conflict over sex determination

Patrice David[1], Cyril Degletagne[2], Nathanaelle Saclier[3] Aurel Jennan[2], Philippe Jarne[1], Sandrine Plénet[2], Lara Konecny[2], Clémentine François[2], Laurent Guéguen[4], Noéline Garcia[2], Tristan Lefébure[2*], Emilien Luquet[2*]

[1] CEFE, CNRS, Univ Montpellier, IRD, EPHE, Montpellier, France

[2] Univ Lyon, CNRS, ENTPE, UMR5023 LEHNA, F-69622 Villeurbanne, France

[3] ISEM, CNRS, Univ. Montpellier, IRD, EPHE, Montpellier, France

[4] Univ Lyon, Université Claude Bernard Lyon 1, CNRS UMR 5558, Laboratoire de Biométrie et Biologie Evolutive, Villeurbanne, France

[*] Equal contributions

Corresponding Author : Patrice David, patrice.david@cefe.cnrs.fr

Lead Contact : Patrice David, patrice.david@cefe.cnrs.fr

SUMMARY

Cytoplasmic male-sterility (CMS) is a form of genetic conflict over sex determination that results from differences in modes of inheritance between genomic compartments[1–3]. Indeed, maternally-transmitted (usually mitochondrial) genes, sometimes enhance their transmission by suppressing the male function in a hermaphroditic organism, to the detriment of biparentally-inherited nuclear genes. As a result, these hermaphrodites become functionally female, and may coexist with regular hermaphrodites in so-called gynodioecious populations[3]. CMS has been known in plants since Darwin's times[4], but is previously unknown in the animal kingdom[5–8]. We relate the first observation of CMS in animals. It occurs in a freshwater snail population, where some individuals appear unable to sire offspring in controlled crosses and show anatomical, physiological and behavioral characters consistent with a suppression of the male function. Male-sterility is associated with a mitochondrial lineage that underwent a spectacular acceleration of DNA substitution rates, affecting the entire mitochondrial genome – this acceleration concerns both synonymous and nonsynonymous substitutions and therefore results from increased mitogenome mutation rates. Consequently, mitochondrial haplotype divergence within the population is exceptionally high, matching that observed between snail taxa that diverged 475 million years ago. This result is reminiscent of similar accelerations in mitogenome evolution observed in plant clades where gynodioecy is frequent[9,10], both being consistent with arms-race evolution of genome regions implicated in CMS[11,12]. Our study shows that genomic conflicts can trigger independent evolution of similar sex determination systems in plants and animals, and dramatically accelerate molecular evolution.

RESULTS AND DISCUSSION

Mitochondria are ancient prokaryotes integrated within eukaryotic cells[13]. This association is described as mutualistic because nuclear and organelle genomes cooperate in essential functions, including oxidative phosphorylation. However, mitochondrial genomes are generally inherited through one sex (usually females), unlike nuclear genomes, which are transmitted by both sexes[8], leading to conflicts over sexual reproduction. In animals, including humans, mitochondrial mutations impairing male fertility, but neutral in females, persist in populations because selection on maternally-inherited genes cannot operate in males – a phenomenon termed the "mother's curse"[14–16]. In some plants, some mitochondrial lineages induce CMS, turning hermaphrodites into functional females[1,3]. Indeed, plant mitogenomes are large, rich in noncoding, repetitive sequences, and prone to structural rearrangements[8,17,18] that occasionally give rise to novel genes that suppress the male function[2,19]. Surprisingly, similar systems have never been detected in the many animal phyla that contain hermaphrodites[6–8,17] – in sea anemones, female and hermaphroditic conspecifics coexist within populations, but they likely represent successive stages in sexual development rather than genetic morphs[5]. One proposed explanation for missing animal examples of CMS is that the mitochondrial DNA (mtDNA) in bilaterian animals is more compact and structurally stable than in plants; thus, despite higher point mutation rates (relative to plants), CMS mutants may rarely appear in animals[6,7,20,21]. However, occasionally, animal mitogenomes seem to escape from their usual conservatism. For example, in book lice, a gonochoristic insect (with males and females), highly rearranged, mutated and structurally unstable mitogenomes occur in some lineages characterized by the inability to produce males – and therefore depending on males from other lineages for fertilization[17,22]. One would therefore expect CMS to be possible in some hermaphroditic animals. Here we relate the discovery of the first example of animal CMS in the hermaphroditic freshwater snail *Physa acuta*. In agreement with our expectation, male sterility is associated with a mitochondrial lineage that diverged extremely fast from other lineages within this species, illustrating the power of intra-organism conflict as an accelerator of evolution.

Two extremely divergent mitogenomes coexist within snail populations

Diverged mtDNA was first discovered in *P. acuta* during a survey of COI, a mitochondrial gene commonly used in phylogeography. In a population near Lyon (France) five individuals shared a COI sequence (called mitotype D, for "divergent") with divergence of 24.7% (±0.3%SD) from the remaining 29 individuals (collectively called mitotype N, for "normal", among which average divergence was 0.9±0.8%). Mitotype D is more than 20% divergent from all published COI sequences (from *P. acuta*[23], or any other animal species present in the GenBank repository), while N sequences from Lyon appeared within the expected range of divergence from other *P. acuta*. The divergence between D and N matches that of snail clades separated hundreds of millions of years ago (Figure 1A).

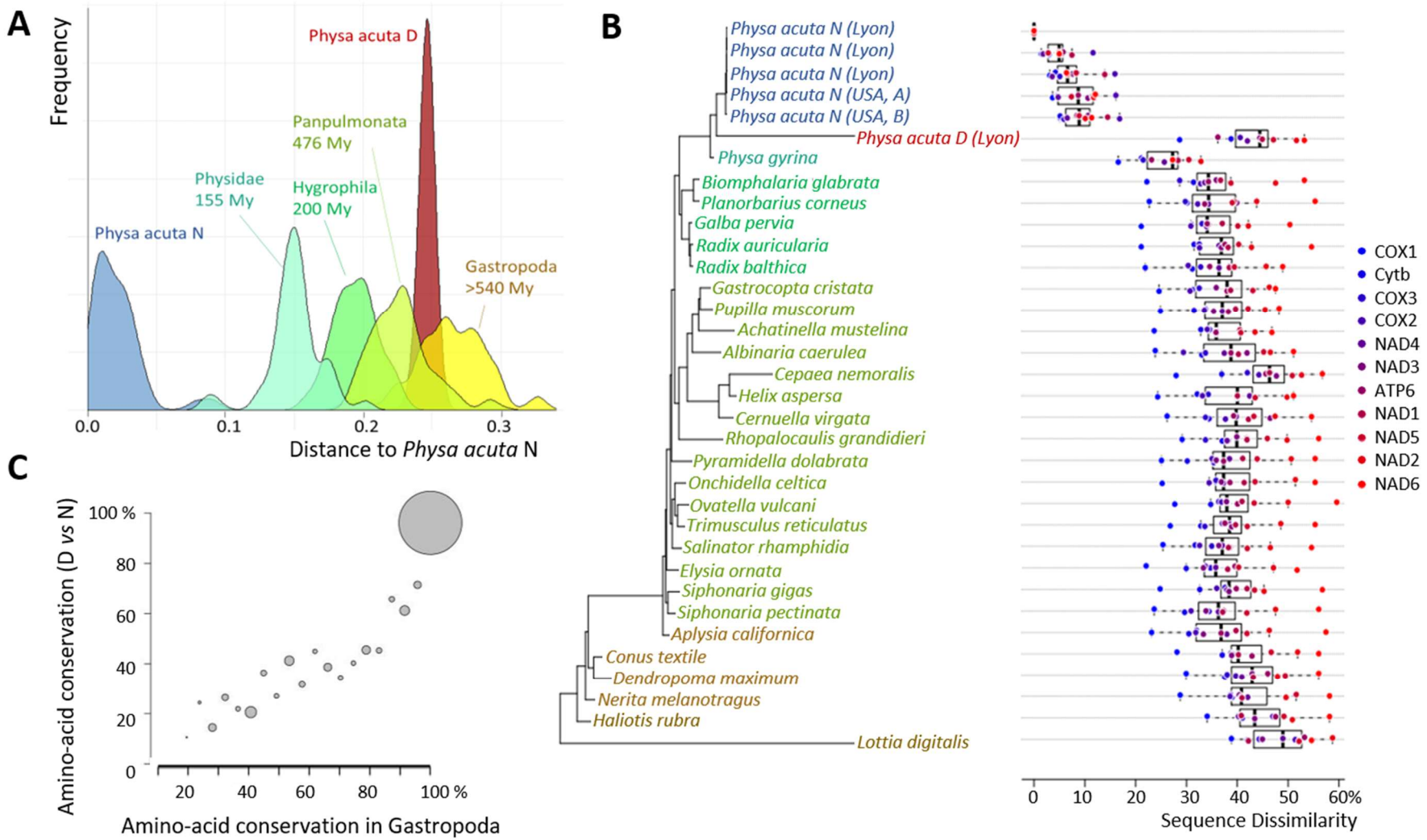
A
Frequency
Physa acuta D
Panpulmonata
476 My
Physidae
155 My
Hygrophila
200 My
Physa acuta N
Gastropoda
>540 My
0.0
0.1
0.2
0.3
Distance to Physa acuta N
B
Physa acuta N (Lyon)
Physa acuta N (Lyon)
Physa acuta N (Lyon)
Physa acuta N (USA, A)
Physa acuta N (USA, B)
Physa acuta D (Lyon)
Physa gyrina
Biomphalaria glabrata
Planorbarius corneus
Galba pervia
Radix auricularia
Radix balthica
Gastrocopta cristata
Pupilla muscorum
Achatinella mustelina
Albinaria caerulea
Cepaea nemoralis
Helix aspersa
Cernuella virgata
Rhopalocaulis grandidieri
Pyramidella dolabrata
Onchidella celtica
Ovatella vulcani
Trimusculus reticulatus
Salinator rhamphidia
Elysia ornata
Siphonaria gigas
Siphonaria pectinata
Aplysia californica
Conus textile
Dendropoma maximum
Nerita melanotragus
Haliotis rubra
Lottia digitalis
COX1
Cytb
COX3
COX2
NAD4
NAD3
ATP6
NAD1
NAD5
NAD2
NAD6
0
10
20
30
40
50
60%
Sequence Dissimilarity
C
Amino-acid conservation (D vs N)
100 %
80
60
40
20
0
20
40
60
80
100 %
Amino-acid conservation in Gastropoda

Figure 1 | The D mitotype in *P. acuta* is exceptionally divergent from conspecific individuals. A) Distributions of pairwise DNA distances (fraction of non-identical nucleotides) at the COI mitochondrial gene in snails. All pairs include one individual of the N mitotype of *P. acuta*. Colors indicate whether the second individual belongs to *P. acuta* mitotype N, or to *P. acuta* mitotype D, or to another species within Physidae, or to another family within Hygrophila, and so on with higher clades. The approximate age of the common ancestor of each clade is indicated (based on references[44–46]) in million years (My). Data include 304 sequences from Genbank (Data S1A) as well as 34 new sequences of *P. acuta* (5 D + 29 N) from Lyon. **B)** Snail phylogeny based on complete protein-coding mitochondrial sequences (colored according to taxonomical position as in Figure 1A). Nucleotidic distance with the top *P. acuta* individual (N mitotype), taken as reference, is indicated for 11 mitochondrial protein-coding genes (with median and quartiles). Data include four new complete mitogenomes of *P. acuta* (3 N + 1 D) from Lyon (one representative of each of the four subtypes found among 21 sequenced individuals), and 30 published gastropod sequences (Data S1B), including two *P. acuta* (N type, USA). The Patellogastropod *Lottia digitalis* is used as outgroup. **C)** Amino-acid conservation between D- and N- mitotypes of *P. acuta* (% of identical amino acids) as a function of conservation in Gastropoda (estimated at all codon positions as the frequency of the most common amino acid across all taxa from Figure 1B, and then pooled in 20 equidistant classes). The positive correlation shows that aminoacid changes between D and N lineages are rarer at phylogenetically conservative sites (those with high frequency of most common amino acid). Circle diameter is proportional to sample size (N=848 sites for the largest circle). See also Data S1, Table S1 and Figures S1, S2.

Similar results were obtained for another mitochondrial gene, encoding the 16S rRNA (see Figure 2A). We then sequenced and assembled complete mitogenomes of 21 *P. acuta* individuals from Lyon and confirmed that abnormal D-N divergence was not restricted to these two genes. All mitochondrial coding sequences were affected, with a startling median divergence, between the D and N haplotypes, of 44.4% for nucleotides (range 28.6-53.2%) and 45.2% for amino acids (17.1- 68.1%) (Figure 1B). This exceeds previous estimates of intraspecific mtDNA divergence not only in *P. acuta* (up to 11.5%[23,24]), but also in any other metazoan we know of (Table 1). Furthermore, although D and N mitogenomes have similar lengths (14.4 Mb), they differ by a four-gene inversion (Figure S1, Table S1). Smaller structural variants also occurred among N mitotypes (unsurprisingly since *P. acuta* mtDNA is known to be highly rearranged compared to related snails[24]).

Mitogenome-wide increase in mutation rates in the divergent lineage

Several hypotheses could potentially explain exceptional sequence divergence. First, divergent mtDNAs might coexist within individuals, e.g. due to transmissible cancers[25], or coexistence of paternally and maternally transmitted mitochondria, as in some bivalves[26]. However, a single mitotype was retrieved per individual, ruling out such heteroplasmy. Moreover, PCR tests on 108 laboratory-reared snails confirmed maternal inheritance, as maternal sibs always had identical mitotypes. Alternatively, the D mitotype could have been captured from a distant species by introgression. However, based on 29 available gastropod mitogenomes, including two *Physidae,* the D mitotype grouped with other *P. acuta* (Figure 1B), indicating a recent origin. Phylogenies based on COI and 16S sequences (which are available in many more *Physidae*) also placed the D mitotype within the *Physa* genus (Figure S2). Its exceptional divergence therefore results from an mtDNA-wide acceleration of substitution rates rather than from an extremely old age. The number of substitutions accumulated in protein-coding genes in the branch leading to the D mitotype, estimated using the YN98 model of codon evolution, was 4.5 times that of the N branch (Table S2; more complex models, incorporating non-stationary codon frequencies and variable selection among sites, return values of 4.87 to 8.71). The actual ratio may be higher if acceleration started after the N-D split.

High DNA substitution rates can result from elevated mutation rates or from more frequent selective fixation of adaptive mutations. Selection should leave a “footprint” of high ratios of non-synonymous to synonymous substitutions (dN/dS). However, dN/dS was low in both D and N (0.047 vs. 0.046), and so were ratios of radical/conservative amino-acid changes (Kr/Kc) (0.767 vs. 0.749) (Table S2). Hot- and cold-spots of non-synonymous changes in the D mitotype were the same as in 28 gastropod species (Figure 1C). Substitution rates in nuclear sequences encoding mitochondrial proteins, retrieved from 21 individual transcriptomes, were also low, similar to those of other nuclear genes (median nucleotide divergence: 0.58% *vs.* 0.57%; amino-acid dissimilarity: 0.12% *vs.* 0.30%; Figure 2B). Overall, this suggests that divergence in D mitogenomes reflects an elevated mitochondrial mutation rate rather than selection on mitochondrial functions.

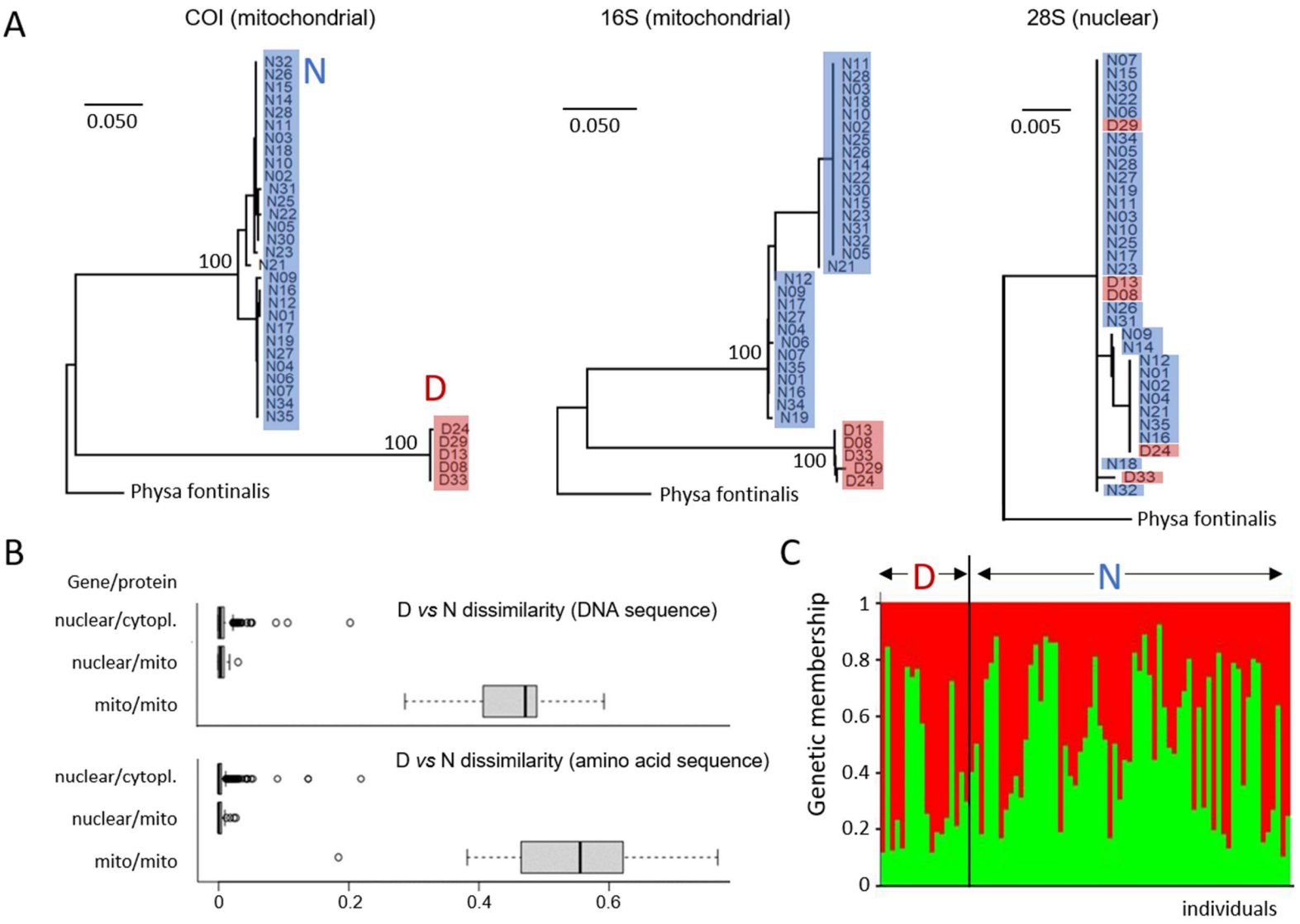
A
COI (mitochondrial)
16S (mitochondrial)
28S (nuclear)
0.050
0.050
0.005
N
D
100
100
100
100
Physa fontinalis
Physa fontinalis
Physa fontinalis
B
Gene/protein
nuclear/cytopl.
nuclear/mito
mito/mito
D vs N dissimilarity (DNA sequence)
D vs N dissimilarity (amino acid sequence)
0
0.2
0.4
0.6
C
D
N
Genetic membership
1
0.8
0.6
0.4
0.2
0
individuals

Figure

2 | Nuclear and mitochondrial patterns of genetic similarity are strongly discordant in a snail population. A) Maximum-likelihood phylogenetic trees of mitochondrial (COI and 16S) and nuclear (28S) genes from *P. acuta* individuals of the Lyon population, highlighted in red (D mitotype) or blue (N mitotype), showing discordant patterns in mitochondrial versus nuclear genes. Bootstrap scores are indicated for the main clades, and *Physa fontinalis* was used as an outgroup. Note the difference in scale between the 28S tree and the other two. **B)** Pairwise divergences between D and N coding sequences (uncorrected p-distances), obtained from transcriptomes, classified according to gene localization (mitochondrial *vs.* nuclear DNA) and to cellular localization of the corresponding protein (mitochondrial *vs.* cytoplasmic). Boxes indicate median and interquartile, whiskers indicate the range (*i. e.* all values within ±1.5 interquartile from the box); dots are outliers (*i. e.* outside the range). **C)** Barplot of membership to two genetic clusters based on nuclear microsatellite loci. Each vertical bar indicates the fraction of genome originating from clusters 1 (red) and 2 (green) in one individual from the Lyon population. Individuals with D and N mitotypes are represented on different sides, and randomly ordered within each mitotype. See also Table S2 and Figure S3.

Divergent snails are sexually compatible with congeners but male-sterile

We sequenced a nuclear gene (28S) in our original sample of 34 snails, and obtained many nuclear coding sequences from a set of 21 transcriptomes. Unlike mitochondrial sequences, nuclear sequences did not form separate clusters of D and N individuals, nor did they show unusual divergence (Figures 2A and 2B). Genetic differentiation at hypervariable nuclear microsatellite markers between D and N individuals from Lyon was small and non-significant (F_{st} = 0.004, P = 0.096) and microsatellite-based genetic clusters (using the STRUCTURE algorithm) did not separate N and D groups (Figure 2C). These data suggest free genetic exchange between the nuclear backgrounds of D and N.

We tested whether D and N individuals could interbreed by pair-mating each of 103 first-generation snails from Lyon with a reference *P. acuta* individual from an albino laboratory culture from Montpellier (300 km South of Lyon). Albinism, a monogenic recessive trait, served as marker of snail origin, and all albino individuals had the N mitotype. In these assays, N snails from Lyon frequently copulated with their mates, taking both male and female roles. Subsequently, both partners laid eggs and nearly all hatchlings from albino mothers were pigmented (sired by the pigmented Lyon individual), while hatchlings from N Lyon mothers were sired by albinos (all were heterozygous, as revealed by back-crossing three offspring per mother with albinos, which invariably produced mixed albino and pigmented progeny). In contrast, D snails exhibited much reduced male activity, often none at all (Figure 3A). Out of 50 albinos paired with D snails, 46 laid no eggs, or produced only albino (self-fertilized) hatchlings (Figure 3C). However, female behavior and fertility of D snails were normal (Figures 3B, 3D), and they produced many offspring sired by albino mates (the heterozygous status of offspring was checked by backcrossing, as previously). Overall, although D and N individuals appeared sexually compatible and fertile as females, the male functions of D individuals were defective. D snails indeed had small seminal vesicles containing very little or no sperm (Figures 3E, 3F, Data S2F). Apart from this, dissections did not reveal any striking difference in reproductive anatomy : in both D and N snails reproductive organs were all placed as in the *Physa acuta* reference description[27].

Defective expression of male behavioral and fitness traits was not restricted to the context of the experiment, as it was confirmed by additional assays (Data S2) in various contexts: (i) pair-crosses with non-virgin mates, a situation where male copulations and paternities are harder to obtain, but more representative of natural settings, where multiple mating and sperm competition are frequent (Data S2A, S2C); (ii) pair-crosses of individuals from Lyon with one another, thus excluding any sexual incompatibility due to allopatric divergence between Lyon and Montpellier (Data S2B, S2D); (iii) isolated snails, showing that D individuals not only lacked the ability to fertilize partners, but also to self-fertilize their own eggs (Figures 3G, 3H, Data S2E). In summary, the D mitotype is associated with near-complete male sterility, and D snails depend on N partners to fertilize their eggs. Both mitotypes coexist in Lyon (14% D *vs.* 86% N), indicating that D individuals can readily find N partners in nature.

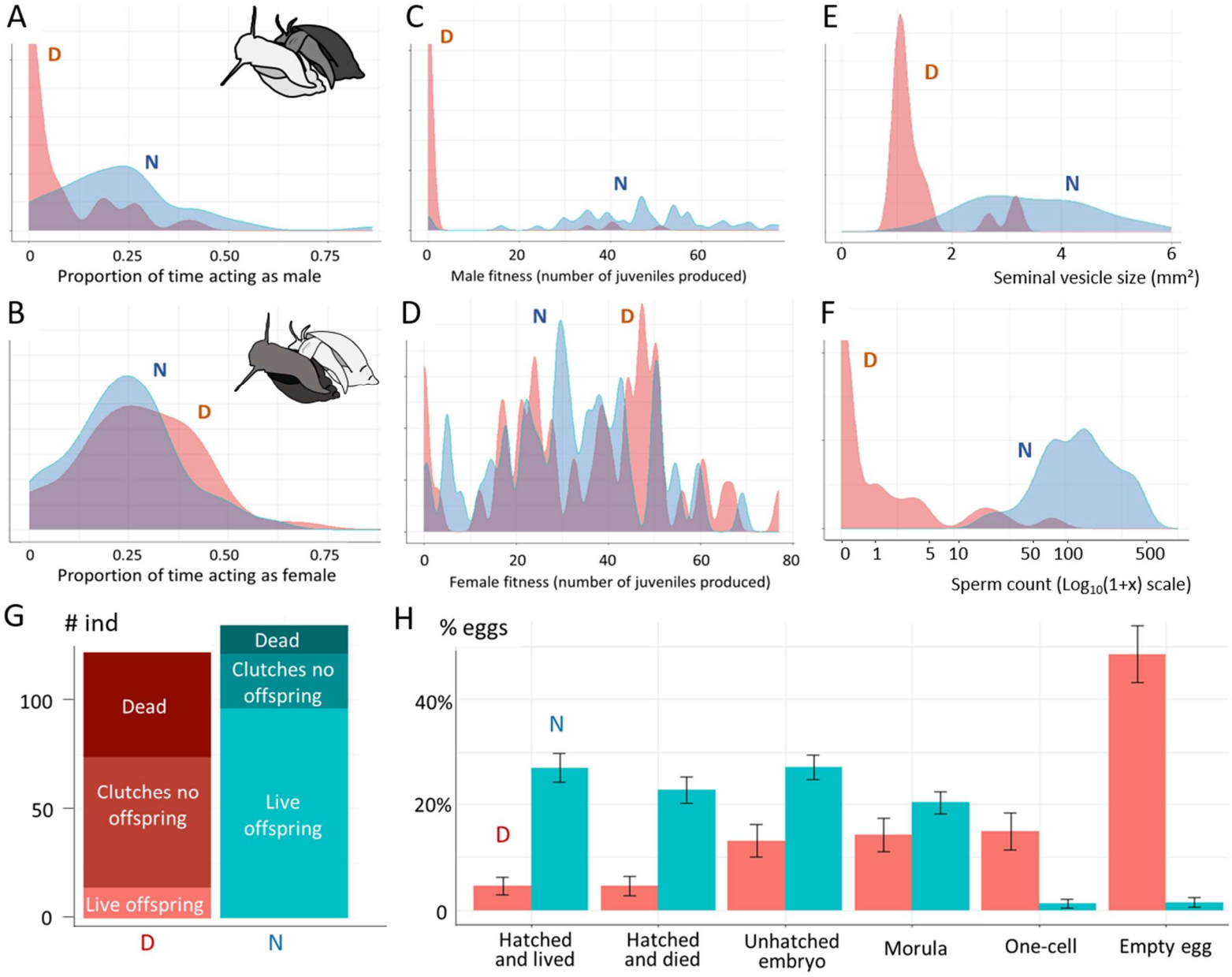
A
D
N
0
0.25
0.50
0.75
Proportion of time acting as male
B
N
D
0
0.25
0.50
0.75
Proportion of time acting as female
C
D
N
0
20
40
60
Male fitness (number of juveniles produced)
D
N
D
0
20
40
60
80
Female fitness (number of juveniles produced)
E
D
N
0
2
4
6
Seminal vesicle size (mm²)
F
D
N
0
1
5
10
50
100
500
Sperm count (Log10(1+x) scale)
G
ind
Dead
Clutches no offspring
Live offspring
100
50
0
D
N
H
% eggs
40%
20%
0
D
N
Hatched and lived
Hatched and died
Unhatched embryo
Morula
One-cell
Empty egg

Figure 3 | The D mitotype is associated with male-sterility. A, B) Distributions of time spent in male and female behavior by D and N individuals, paired with virgin partners, in 45-mn assays. Drawings illustrate mating positions of focal individual (dark) and mate (light), viewed from below (top snail acts as male, with penis introduced under the partner's shell; each snail is approximately 1 cm long). **C)** Male fitness (number of juveniles produced by partner and sired by focal snails). **D)** Female fitness (juveniles produced by focals). **E)** Size of the seminal vesicle (sperm storage organ) and **F)**, sperm counts (1/1000 of the total seminal vesicle content) in adult, virgin individuals. *P*-values are from linear models testing the mitotype effect (D vs N) (reported in full in Data S2). **G)** Reproductive traits of isolated virgin snails of N and D types: Numbers of individuals (N ind) that produced live (self-fertilized) offspring, laid egg capsules that failed to produce live offspring, or died before laying eggs (we waited for each individual to either lay eggs or die, those that died first were usually very old, i.e. they had survived without laying eggs for a long time). **H)** proportions of eggs laid by isolated D and N snails reaching given developmental stages, 14 days after egg collection (+/-SEM based on 121 clutches from N snails and 74 clutches from D snails). 'Hatched and lived' are free-moving hatchlings alive, 'hatched and died' were dead shells found in the bottom of boxes (probably underestimated, as some may have been lost), 'unhatched embryo' were found dead in the egg envelope while presenting a distinctive body plan, 'morula' stopped developing at a stage with several cells but morphogenesis had not begun, 'one-cell' eggs looked initially normal (with visible nucleus) but did not undergo cleavage, and 'empty eggs' were laid without visible nucleus at all (i.e. egg envelopes without visible cell content). See also Data S2.

Species	Taxonomic group	Reproduction	Reference	Within/among populations	Divergence			
					COI	16S	Cyt.b	mitogenome
Physa acuta	Mollusks	hermaphroditic	This study	within	28.6	15.4(420bp) 23.0 (915bp)	38.8	28.6-53.2 (median 44.4)
Cepaea nemoralis	Mollusks	hermaphroditic	Thomaz et al 1996 [28]	within		12.9 (300bp)		
Frigidoalvania brychia	Mollusks	gonochoric	Quattro et al 2001 [29]	among		25.8 (130bp)		
Goniobasis proxima	Mollusks	gonochoric	Dillon & Frankis 2004 [30]	among	16.9	16.6 (530bp)		
Arion subfuscus	Mollusks	hermaphroditic	Pinceel et al 2005 [31]	among		20.0 (450bp)		
Spadella cephaloptera[a]	Chaetognaths	hermaphroditic	Marletaz et al 2017 [32]	within	18			
Sagitta elegans	Chaetognaths	hermaphroditic	Marletaz et al 2017 [32]	within	20.8			
Lumbricus rubellus	Annelids	hermaphroditic	Giska et al 2015 [33]	within	17.5[c]			
Cordylochernes scorpioides	Arachnids	gonochoric	Wilcox et al 1997 [34]	among	13.8			

Tigriopus californicus	Copepods	gonochoric	Burton et al 2007 [35]	among	17			10-25
Liposcelis bostrychophila[ab]	Hexapods	gonochoric[b]	Perlman et al 2015 [17]	within	23.4	21.1 (1000bp)	23.2	19.9-46.9
Ceratosolen solmsi[a]	Hexapods	gonochoric	Xiao et al 2011 [36]	within	9.2		15.3	
Galaxias maculatus	Teleost	gonochoric	Waters & Burridge 1999[37]	among		5.8 (520bp)	14.6	

Table 1 | Cases of high within-species mtDNA divergence in metazoans. Overview of studies reporting a large divergence of mitochondrial genes within animal species, either within or among populations. We report the reproductive system (hermaphroditic or gonochoric) and the divergence (uncorrected p-distance in %) at COI, 16S and cytochrome b genes, and/or for the entire mitogenome, depending on availability. Note that 16S data are difficult to compare, as studies bear on different sub-parts of the gene, of various lengths (in brackets), often difficult to align. For *P. acuta* (this study), we provide two estimates for 16S: one based on an easily aligned part used for the phylogeny (420 bp; likely to be an underestimate as very divergent parts are the hardest to align); the other on 915 bp aligned from the complete genomes in the transcriptomes (likely an overestimate). [a] In these studies, structural rearrangements in mitogenomes are also reported. [b] In this species, some genotypes perpetuate themselves as clonal females, paternal genetic material being eliminated before meiosis (not transmitted). [c] mtDNA fragments COI and ATP6 were concatenated.

Fast mitogenome evolution and genomic conflicts over male reproduction

The D mitotype in *P. acuta* is the first example of CMS in hermaphroditic animals. It coincides with an extreme intraspecific divergence of the mitogenome, due to an elevated mutation rate, and structural rearrangements. This association is unlikely to be fortuitous. In plants, although most known male-sterility genes arise by *de novo* structural rearrangements in the mtDNA[8,17,28], increases in mtDNA mutation rates occasionally accompany CMS. Clades in the *Plantaginaceae* and *Caryophyllaceae*, where CMS is frequent, underwent spectacular increases in mitogenome substitution rates[9,10,29,30], and very divergent mitochondrial haplotypes often coexist in species showing CMS[31–33]. Although CMS in plants may not initially arise by point mutation, high substitution rates may help it persist over evolutionary time, as male-sterile mitotypes have to keep up with the constant evolution of nuclear genes restoring male fertility[11,19]. The main family of plant restorer genes, encoding post-transcriptional regulators of mtDNA expression, bears traces of such an arms-race situation[12]. A similar process may occur in hermaphroditic animals, with nuclear genes quickly neutralizing mitochondrial CMS mutations, unless the mtDNA evolves fast enough to escape restoration.

Support for this hypothesis comes from studies showing that in animals, many mutations in mitochondrial genes of the OXPHOS system are deleterious to male fertility (especially sperm viability and motility), but neutral[34] (or sometimes beneficial[35]) to females. The high energetic needs of spermatogenesis, and low number of mitochondria per sperm, may make male gametogenesis particularly sensitive to alterations in mitochondrial metabolism[8,28,34]. Male-harming mutations can invade populations by genetic drift (if neutral to females) or under selection, if they benefit females. Preservation of male fertility then depends on compensatory evolution of nuclear genes[34]. This process could explain why interspecific hybridization often generates cyto-nuclear incompatibilities and male sterility[36] and why highly mutated, structurally instable mitogenomes co-occur with nuclear genomes transmitted only via females, in book lice[22] (note that in these insects, males are required to fertilize females' eggs but paternal chromosomes are excluded from females' germlines[37]).

In hermaphroditic animals, such as *P. acuta*, each individual carries both sexual functions, and male-suppressing mutations may increase female fitness more often than in gonochoristic species. First, male sterility prevents self-fertilization, thus avoiding the potential cost of inbreeding depression[38] (which is~~is~~ very high in *P. acuta*[39]). Second, stopping sperm production may directly free resources for growth or egg production[21,40]. In our experiments, male-sterile snails were heavier than male-fertile ones (P = 0.002, Data S2G). They also produced ~10% more eggs and offspring, but owing to large individual variance this difference was not significant (P>0.05; Data S2B, S2D). Models of CMS evolution show that even tiny female advantages allow mitochondrial male-sterilizing alleles to increase in frequency[1,3]. In plants, such advantages are generally present[40], although environment-dependent and often hard to detect. Further experiments may find conditions in which they are detectable in *P. acuta* too. More generally, a complete comparison of quantitative anatomy, histology, and gene expression between N and D snails will be needed to fully characterize the extent of phenotypic differences associated with male-sterility in *Physa acuta*. In particular, an intriguing result we obtained is that a few snails within a D family were not totally male-sterile. These snails were too few to claim that nuclear restoration of male fertility exists in this species, but their belonging to the same family is certainly suggestive of this possibility.

Non-synonymous to synonymous substitution ratios provide no evidence for positive selection in the *P. acuta* D haplotype. Purifying selection (acting on survival or female reproduction) seems to have preserved the essential mitochondrial functions during divergence, as none of the mitochondrial genes has degenerated and conserved sites have been maintained. However, as mitogenomes do not recombine, favorable mutations, including male-sterility ones, may go undetected among many neutral mutations captured within the successful mtDNA lineages. The very low diversity found within the D haplotype is consistent with such selective sweeps. Currently, the high number of non-synonymous substitutions makes it impossible to pinpoint individual mutations affecting male function, especially as multiple mutations may have accumulated over time. In addition, as in most known examples of CMS, the coincidence of mitochondrial mutations and male-sterility does not demonstrate direct causality. The existence of male-sterilizing mutations somewhere in the D mitogenome is however, for now, the most parsimonious explanation, given that such mutations have been functionally characterized in mitochondrial genes of plant taxa and gonochoric animals, and that we currently know of no other maternally-transmitted element that might cause both CMS and fast mitochondrial evolution.

In summary, it is unlikely to be chance that CMS is discovered in hermaphroditic animals more than a century after it was in plants. Detecting male-sterility is not easy in animals, as sperm-producing organs, unlike plant stamens, are concealed within the body and sterility assessment requires dissection or paternity analysis. However the difference between animals and plants may reflect more than ease of detection. CMS may also genuinely be rare in animals if only exceptional conditions allow animal mitogenomes to escape their usual conservatism, enabling them to produce many male-harming mutations and sustain the arms race with nuclear genes. An increase in mtDNA mutability provides such a condition, and, in *P. acuta*, has resulted in an extreme degree of intrapopulation haplotype divergence. Cases of high mitochondrial variation have been reported in other animal hermaphrodites (in snails[41], earthworms[42] and chaetognaths[43]) and are worth testing for CMS. Our study shows that intragenomic conflicts can be powerful accelerators of molecular evolution. Exploring the mechanisms by which conflicts between mitochondria and nuclear genes impact sexual reproduction, will be a fascinating research avenue.

ACKNOWLEDGEMENTS

We thank J.-P. Pointier for dissecting snails for us and sharing his knowledge on snail anatomy, and D. Charlesworth and three anonymous reviewers for commenting the manuscript. This work was funded by CNRS, the MINIGAN (ANR-19-CE02-0017) and the EUR H2O'Lyon (ANR-17-EURE-0018) grants from the french National Research Agency (ANR) and Université de Lyon (UdeL). We dedicate this article to the dear memory of Violette Sarda, who accompanied us through 20 years of snail research at the CEFE.

AUTHOR CONTRIBUTIONS

P.D., E.L. and T.L. supervised the study. C.D., N.S., L.K., C. F., T.L., N.G., S.P., L.G. generated and analysed the sequence data; P.D. performed and analysed the microsatellite and

breeding experiments. A.J. performed sperm counts and seminal vesicle measurements. P.D., C.D. and E.L. wrote the manuscript with additional input from all other co-authors.

DECLARATION OF INTERESTS :

The authors declare no competing interests

STAR METHODS

RESOURCE AVAILABILITY

Lead contact

Further information and requests for resources and reagents should be directed and will be fulfilled by the lead contact, Patrice David (patrice.david@cefe.cnrs.fr)

Materials availability

This study did not generate new unique reagents.

Snail strains used in this study are maintained in CEFE, Montpellier and available upon request to the lead contact.

Data and Code availability

All sequences, RNA-seq data and assembled mitogenomes generated in this study have been deposited in the ncbi repositories Genbank and BioProject, and are publicly available as of the date of publication. Accession numbers are listed in the Key Resources Table. All other data reported in this paper are available from the lead contact upon request.

This paper does not report original code.

Any additional information required to reanalyze the data reported in this work paper is available from the Lead Contact upon request.

EXPERIMENTAL MODEL AND SUBJECT DETAILS

Thirty-eight *Physa acuta* G0 individuals were sampled in March 2015 in a backwater from the Rhone River in Lyon, France (N 45°48'05.3", E 4°55'26.1"), kept overnight in a 10 L-aquarium, then isolated in separate boxes (75 mL), where they layed egg capsules for one week. After egg hatching, we collected and raised individually *ca*. 10 G1 offspring from each G0 mother. Within each maternal family (hereafter, matriline), some offspring were frozen to extract DNA for molecular analyses and others were kept alive. We later collected additional G0 individuals in the same site, in September 2016 (N=108) and in February 2017 (N=29), and used them to found new matrilines (see below). 21 such matrilines, each derived from a single G0 ancestor, have been propagated by maternal descent to this day, using albino individuals from Montpellier as sperm donors at each passage of generation.

We also used a laboratory albino population of *Physa acuta*, maintained as a large outbred population for over 50 generations, and initially derived from a mix of ten natural populations from Montpellier[47]. Albinism is due to a single recessive allele. It was initially observed in a few individuals in the mixed population, which we multiplied; the resulting albino population was then re-introgressed four successive times by >50 parents of the mixed population to ensure a large genetic variability. Since then the albino population has been maintained in large numbers (>200).

METHOD DETAILS

COI, 16S and 28S sequences

The mitochondrial genes COI and 16S, and the nuclear 28S, were amplified (primers in key resource table) and Sanger-sequenced in one second-generation offspring of each of 34 matrilines, out of the 38 obtained in 2015. A COI dataset was assembled using our sequences and 304 additional COI sequences retrieved from GenBank, of *P. acuta* and other snails along a gradient of phylogenetic distance from *P. acuta* (Data S1A). Uncorrected nucleotidic p-distances between all pairs of sequences were computed to generate Figure 1a, in which we represented the distribution as a smoothed-density function using R-package ggplot2 3.3.5[48] geom_density() function with bandwidth 0.005, vertical scale adjusted to fit the highest peak. Ages of clades in Million years (My) were obtained from references[44–46]. We then generated phylogenetic trees for each of the three genes with our 34 sequences, using *Physa fontinalis* (GenBank accessions: COI: FJ373018; 16S: AY651227; 28S: AF327540) as outgroup (Figure 2A). We retrieved 103 additional COI and 16S sequences of the Physidae family (when both were available for the same accession), as well as outgroups in the Hygrophila clade from the GenBank repository (Data S1). The two genes were concatenated, and we built a phylogenetic tree, based on our sequences and those from GenBank (Figure S2). Phylogenetic trees were made using PhyloBayes[49] under the CAT-GTR+G+I model.

PCR test to distinguish D and N mitotypes

The divergence in COI sequence between D and N mitotypes allowed us to design primers specific to each of the two mitotypes (see key resources table), within the 705 bp fragment amplified using the classical "Folmer" primers[50]. We designed a simple PCR mitotype diagnostic as follows (see Figure S3). Each sample was amplified with two separate PCR mixes. The first mix combined the Folmer primers and the D-specific internal primer, and amplified a long fragment (705 bp) in N individuals and a short one (604 bp) in D individuals (in which the amplification of the long fragment was blocked by the internal primer). The second mix combined the Folmer primers and the N-specific internal primer and produced the opposite pattern (long fragment in D and short fragment in N individuals). The PCR products of the two mixes were run side by side on standard agarose gels to identify mitotypes based on band patterns (short-long versus long-short). This test was performed on at least one individual of each matriline obtained in 2015-2017 from the Lyon population, including all the parents used in phenotypic assays (see below) and two to five of their maternal sibs (maternal sibs always showed identical patterns). We also used it to check that individuals of the albino laboratory population were all of type N (30 individuals tested).

Analysis of population structure with microsatellite markers

We genotyped 83 G1 individuals (of which 18 came from five D-mitotype matrilines, and 65 from 33 N-mitotype matrilines, obtained in 2015 and genotyped by the above-mentioned PCR test and/or COI sequencing) using seven microsatellite (nuclear) markers (AF108762, AF108764, Pac1, Pac2, Pasu1-11, Pasu1-2, Pasu1-0) developed in *P. acuta*[51,52]. We estimated population differentiation between the two groups using the *Hierfstat* package in R[53]. Because of the matriline structure within each mitotype, the differentiation between the two mitotypes was estimated as the among-mitotype component of molecular variance in a hierarchical model with three levels: mitotype, matriline within mitotype, and individual within matriline. We also used the clustering algorithm STRUCTURE[54] with K = 2 and no prior information on mitotype, in order to check whether microsatellite data formed two genetically distinct clusters matching the D and N mitotypes.

Complete mtDNA sequences

A subset of 21 G1 matrilines from the Lyon population were used to obtain whole-body transcriptomes from which we assembled complete mtDNA sequences**.** Based on PCR tests, we chose 11 D matrilines (1, 7 and 3 from the 2015, 2016 and 2017 samples respectively), and 10 N matrilines (7 and 3 from 2016 and 2017 respectively), and analyzed one adult individual per matriline. In most bilaterian animals, including *P. acuta*, the mtDNA molecule is circular and transcribed in long polycistronic RNA, a characteristic that facilitates genome assembly based on transcriptomes. Total RNA was isolated using TRI reagent (Molecular Research Center). Extraction quality was checked on a Bioanalyser RNA chip (Agilent Technologies), and RNA concentrations were estimated using a Qubit fluorometer (Thermo Fisher Scientific). The first Illumina library was prepared from 600 ng total RNA using the TruSeq™ RNA Sample Prep Kit, the following 20 librairies with the NEBNext Ultra II RNA Library Prep Kit together with the NEBNext Poly(A) mRNA Magnetic Isolation Module. Libraries were paired-end sequenced on a HiSeq2 sequencer (Illumina) using 100 cycles at the Genomeast plateform IGBMC (Illkirch, France) or on a MiSeq sequencer using 150 cycles at Biofidal, (Vaulx-en-Velin, France). Adapters were clipped from the sequence, low-quality read ends were trimmed (phred score < 30), and low-quality reads were discarded (mean phred score < 25 or remaining length < 19 bp) using *fastq-mcf* of the *ea-utils* package[55]. Transcriptome was *de novo* assembled using Trinity[56]. Open reading frames (ORF) were identified with TransDecoder (http://transdecoder.github.io/). For each assembled component, only the longest ORF was retained. Additional published transcriptomes from the freshwater snails *P. acuta*, *Physa gyrina* and *Biomphalaria glabrata*[57] were used to determine gene families and compared with transcriptomes of Lyon individuals. Gene families were delimited using all against all BLASTP[58] and SiLiX[59]. SiLiX parameters were set to maximize the number of 1-to-1 orthologous gene families ($i = 0.5$ and $r = 0.6$). Protein sequences and CDS were aligned using Prank[60] and pairwise similarities (uncorrected *p*-distance) were assessed using the phangorn v2.4.0[61] and ape[62] packages in R.

Mitogenome assembly and comparison among gastropods

Long mitochondrial DNA sequences were assembled using MITObim[63] from paired-end transcriptome reads and known mitochondrial genes from *P. acuta* as seed (NC_023253.1).

The reconstruction of the entire mitogenome was realized by assembling these long sequences using Seaview. MITOS webserver[64] was used to annotate mitochondrial protein coding genes, ribosomal and transfer RNA. We assembled the mitogenome of *P. gyrina* with the same procedure using published RNA-seq reads (SRA database on NCBI, accession SRX565294). The absence of N-mitotype reads in D-mitotype transcriptomes of *P. acuta* (*i.e.* absence of heteroplasmy) was checked using BLASTP[58]. An additional N-mitotype individual (sampled in a population near Lyon, Vorla (N 45°48'46.6, E 4°57'53.6"; 2020/09/08) was later sequenced with Nanopore technology which provides longer fragments (facilitating the assembly). We included it to provide a comparison with assembly from transcriptomes – a consistent length and gene order between transcriptome- and Nanopore-based sequences would confirm that assembly is not subject to some form of methodological bias. The nanopore-sequenced individual was flash-frozen with liquid nitrogen, crushed with a pestle then ground twice for 45 sec using a ball mill grinder (Retsch MM-200). DNA was extracted using the Qiagen Blood & Cell Culture DNA Kit (Genomic-tip 20/G #13323), following the manufacturer specifications, including a 30 min RNAse step and a 2 hr protease step. Short DNA fragments were depleted using the Circulomics Short Read Eliminator Kit (#SS-100-101-01). Starting from 2.7 µg DNA, the MinION library was prepared following Nanopore specifications using a SQK-LSK109 Ligation Sequencing Kit, and run on a MinION flowcell (R9). This run produced 1.3 Gb of data with a N50 of 20 kb. The basecalling was done with Guppy (version 4.0.15) and reads were assembled with Flye version 2.8.1-b1676[65]. One contig was identified as the mtDNA sequence, as it was circular, of length 15405, contained all the mitochondrial genes, and was syntenous to previous RNA-seq assemblies.

We retrieved the mitochondrial genomes of 26 more gastropod species available in GenBank (including 22 Heterobranchia, the sub-class to which *P. acuta* belongs, and four other species from more distant groups). As ATP8 and NAD4L were not available in all species, the analysis was restricted to 11 coding sequences (CDS), which were aligned using Prank software[60]. All sequences were compared to the N mitotype of *P. acuta* in a pairwise fashion using the ape[62] and seqinR[66] packages in R. Sites ambiguously aligned were removed with Gblocks[67] and the CDS were concatenated and used in phylogenetic analysis. Phylogenetic trees were built with PhyloBayes[49] under a CAT-GTR+G+I model. Two independent chains were run, and were stopped after checking for convergence with the tracecomp program included in PhyloBayes (effective sample size > 50 and discrepancy between chains < 0.3 for all statistics). Chains were stopped after 98755 generations (40000 generations were excluded as burn-in) and sampled each 10 generations, resulting in 11750 trees. To ensure no polytomies a threshold of 10% was set to obtain the majority consensus tree. FigTree v1.4.2[68] was used to edit the phylogenetic tree.

A subpart of this tree, keeping only *P. acuta, P. gyrina* (the closest available outgroup to *P. acuta*) and *Biomphalaria glabrata* (used as outgroup) was used to estimate nonsynonymous (dN) and synonymous (dS) substitution rates, as well as, among nonsynonymous substitutions, the ratio of radical to conservative amino-acid changes (Kr/Kc) in the branches leading to the D and N mitotypes from their common ancestor, under the YN98 codon model. The parameters of the YN98 model were estimated with bioppml[69], and the dN, dS, dN/dS, and Kr/Kc were

estimated using substitution mapping with mapNH[70] (newlik branch). This was done both for each of the 11 CDS separately and for a concatenation of them all.

Morphological comparison between individuals with D and N mitotypes

The internal anatomy (especially the morphology of the reproductive apparatus) is the main criterion for delimitating species in freshwater snails. The anatomical description serving as reference for *P. acuta* has been made based on topotypic specimens[27]. We asked one of the authors of this description (J.-P. Pointier) to examine and dissect 24 N and D individuals, each from a different matriline (without prior knowledge of mitotype). He classified all specimens as standard *P. acuta* without noticing any anomaly in the reproductive apparatus (see below however, for quantitative differences in sperm production and seminal vesicle size, that could not be detected visually).

Behavioral and reproductive traits of individuals with D and N mitotypes : overview

We measured behavioral and fitness traits on first- and second-generation descendants of snails of the 2017 sample from Lyon. These individuals belonged to 22 matrilines, 11 of each mitotype. The mitotypes were first identified in one G1 offspring per matriline using the PCR assay, and then re-checked in the G2 individuals. No variation in mitotype was detected within matrilines. Experimental individuals, once sexually mature, were paired with partners and sexual behavior was recorded in each pair. After pairing, eggs and juveniles produced by the focal snail were counted to quantify female fitness, while male fitness was estimated based on juveniles produced by the partner and sired by the focal snail. Difference in traits between mitotypes were estimated through (generalized) linear models using *lme4*[71] (see details below). We evaluated behavior and fitness in various conditions, expected to have contrasted effects on the expression of reproductive potential (detailed below), by varying the origin and the mating history of focal snails and their partners. The first pairing took place between virgin snails from Lyon (all pigmented) and virgin albino partners- and is reported in the main text (Figure 3)- the rest in Data S2. After the first pairing, we checked that the juveniles hatched from eggs laid by each focal snail were heterozygous (hence sired by the albino mate) by raising three of them per matriline to adulthood, and then backcrossing them with the albino strain: the offspring produced in these crosses were always a mixture of albino and pigmented, as expected from heterozygous mothers.

Behavioral and reproductive traits of individuals with D and N mitotypes : full report.

Experiments were performed using three sets of snails (hereafter G1-1, G1-2, G2-1), all derived from the same wild-caught (G0) ancestors from Lyon. **The first set (G1-1)** comprises 103 first-generation (G1) individuals (53 N and 50 D) obtained from 22 G0 mothers (11 N and 11 D). Figures 3A-3D (main text) are based on this first set. **A second set (G1-2)** comprises 74 individuals (42 N + 32 D), mostly sibs of the G1-1 individuals, from 21 G0 mothers (12 N, 9 D). **A third set (G2-1)** comprised 256 individuals (134 N, 122 D) obtained from two sources: (i) eggs laid by the G1-1 after they were inseminated by partners from the albino population; (ii) offspring of pair-crosses among G1-2 individuals. As a result, all G2-1 are from Lyon by maternal descent (*i.e.* they inherited their mtDNA from a N or D wild-caught individual from Lyon), but their nuclear genome is either a mix of the Lyon and albino populations ("heterozygous") or 100% from Lyon ("homozygous"). We defined a "matriline" as the set of

all individuals having the same maternal ancestor in the G0 Lyon population, hence the same mtDNA – there were 23 such matrilines (12 N + 11 D) in total, some of them missing in some experiments.

Behavior was recorded (by the same observer, blind with respect to snail mitotype (PD)) in sessions of 45 mn, in which encounters took place between two previously isolated individuals. Individuals were distinguished by either body pigmentation or colored paint marks on the shell, and all sexual interactions were recorded and timed, including sexual attempts (male-acting individual climbs and sits on top of female-acting individual) and copulations (male-acting individual inserts its penis under the shell of the female-acting individual - it is however not possible to ascertain that sperm transfer actually occurs). Note that a marked decrease in sexual activity is commonly observed in experienced, mated snails compared to virgin, inexperienced snails (P.D., pers. obs.).

Observations took place during the first 45mn after the two snails were put together, they were then left together (unobserved) for three days, and re-isolated for three more days to lay eggs in separate boxes in order to measure fitness traits. We then removed the mother snail, counted eggs, let them develop for 14 days, then counted the number of live juveniles and recorded their morph (albino or pigmented). Thus, female fitness traits included the number of eggs and the number of juveniles (called "female fitness") produced in 3 days by the focal individual. Male fitness traits included the number of eggs laid by the focal's partner and the number of juveniles hatched from these eggs and sired by the focal individual (male fitness). Siring success could only be ascertained when the partner was albino (the hatchlings sired by focal individuals were, in this case, pigmented).

G1-1 individuals**.** Each G1-1 individual was paired three times. *First time*: the focal individual was virgin (having been isolated since the juvenile stage) and paired with a virgin albino, and we obtained behavioral and fitness data in each pair. Virgin individuals are usually very eager to mate in both roles, and there was no male-male competition as each individual had a single partner – these conditions normally maximize male fitness. Results of this session are reported in main text Figures 3A-3D. *Second time*: the focal was mated with an albino that had been previously inseminated by other albinos and had stored their sperm (albino mates had been put together in large groups for one week, before the experiment): we recorded only male fitness – the behavior was not assessed for lack of time and manpower. These conditions were more challenging, because of the presence of male-male competition. Indeed, the albino partners had stored sperm from other albinos, with which the focal individual's sperm had to compete for fertilization – male fitness is usually much reduced and more variable in such conditions[72,73]. *Third time*: the focal individuals (from Lyon) were paired with one another, avoiding sib pairs. In this case we monitored behavioral traits only (both partners being nonvirgin and pigmented, there was no way to assess paternities). The aim of this third assay was to check whether behavioral differences observed in the first assay (when individuals were virgin and presumably very eager to mate) (i) persisted in nonvirgin individuals (less eager to mate) (ii) were not specific to interactions between allopatric snails (Montpellier-Lyon) and persisted in sympatric (Lyon-Lyon) pairs. Indeed, as the D mitotype is not known to be present in Montpellier, one could envisage that N and D individuals from Lyon, historically in contact, would have evolved to interact in a way not shared by evolutionarily naive N individuals from Montpellier.

G1-2 individuals**.** These individuals were paired twice successively. *First time*: virgin focals were paired with one another, avoiding sib pairs. Both behavior and fitness data were collected. This allowed us to test sympatric pairs of virgin individuals (a combination not tested in previous assays). Paternity could not be inferred (both parents being pigmented), but as there was no male-male competition, we assumed all eggs laid by one individual to be sired by the other. Previous studies have shown that although *P. acuta* is capable of self-fertilization, individuals outcross nearly all their eggs as soon as they are inseminated[74,75]. In addition individuals not inseminated usually refuse to lay eggs for 2-3 weeks[76,77]. We were therefore expecting that if an individual failed to inseminate its partner, the latter would not lay eggs. *Second time*: the focals were paired with a non-virgin albino and only the behavior was recorded. This assay was performed to compensate the lack of behavioral data from pairs of nonvirgin individuals of Lyon and Montpellier (see G1-1 individuals, second time).

G2-1 individuals**.** Each G2-1 individual was raised entirely in isolation to assess its self-fertilization capacity. As mentioned above, the typical behavior of isolated *P. acuta* is to delay the onset of egg-laying for around 2-3 weeks compared to individuals with access to partners[76,77]. They then lay self-fertilized clutches that have a reduced hatching and survival rate compared to outcrossed clutches (inbreeding depression at this stage is around 50%[78,79]). In our protocol, we waited until each individual either died or started to lay, and when they laid eggs, collected the clutches produced during the first week, then discarded the parent. The collected eggs were then let develop for 14 days, at which point we checked the progeny. We counted how many juveniles were alive at 14 days, how many had hatched and died (dead empty shells), how many had not hatched with development arrested at various stages (one-cell, morula stage, later embryo stage) as well as the number of "empty eggs" (eggs without a visible nucleus at all). These data are reported in the main text Figures 3G, 3H.

The full results of all experiments are reported in Data S2. Overall, these data confirm a strong reduction (though not a complete suppression) of all male behavioral and fitness traits in individuals of mitotype D compared to their N-type counterparts, while female traits did not differ between types, in all conditions tested. A few exceptions have to be mentioned, i.e. two N individuals had 0% paternity while four D individuals obtained paternities (see Figure 3C and Data S2A). Interestingly, all four had been observed copulating as males, and came from a single matriline (D53), which we double-checked by PCR was indeed of mitotype D (a fifth individual from that family had 0% paternity). Seven other D individuals had been observed apparently copulating as males, but still did not get any paternity.

Sperm production

The 22 Lyon matrilines (N and D) used for phenotypic measurements were kept on the long term in the laboratory, propagating them by maternal descent using individuals from the albino stock as sperm donors at each generation. Sixty-four individuals from generation 15 were raised individually (32 individuals of 11 matrilines within both D and N mitotypes, re-checked using the PCR test described above) and sacrificed at age 50 days, without having been mated. Each snail was dissected after being anaesthetized with menthol. The seminal vesicle was extracted, gently squeezed to constant thickness (0.15 mm) between two microscope glass slides, and photographed from above using a camera mounted on a microscope. Its area (mm^2), was estimated from the pictures using IMAGEJ[80], and used as a proxy for its volume (as thickness is constant). The vesicle was then homogenized and vortexed in 100 µl of water, and

sperm counts were made on two independent 0.1 µl aliquots of each extract at 400X magnification, using a hemocytometer.

Quantification and Statistical Analysis

We analysed behavioral and fitness data using Generalized Linear Mixed Models (GLMM) (Poisson or Binomial variables) and Linear Mixed Models (LMM) (continuous variables) implemented in the *lme4* package in R[71]. We used Poisson distributions for count variables, binomial distributions for binary or proportion variables, and Gaussian models for quantitative variables. A 'matriline' random factor was added to account for relatedness among individuals, as well as an 'individual' random factor to account for possible overdispersion in GLMMs. In addition, when two focals were paired, the potential correlation between them was modelled by adding a 'pair' random factor. All tests of fixed effects (mitotype of focal, and when appropriate, mitotype of partner and interaction) were performed using model comparison by Likelihood-ratio (LRT), confirmed by permutation tests for LMMs when heteroscedasticity was suspected (cases with many values near zero). Trait distributions were represented in Figure 3 using ggplot2 v.3.3.5 geom_density() function with default bandwidth except for fitness estimates (Figures 3C, 3D) in which we reduced bandwith to 1, as the default value did not correctly represent the bimodal distribution of male fitness (i. e. the existence of a few individuals with nonzero male fitness among D snails).

Seminal vesicle size and sperm counts were analysed using linear mixed models in the lme4 package in R[71], with mitotype as a fixed factor and matriline as a random factor. For sperm counts, the error distribution was Poisson, an "individual" random factor was added to account for the non-independence of the two counts per individual, and an "observation" random factor (nested within individual) to account for overdispersion. Distributions in Figures 3E, 3F were made with the ggplot2 geom_density() function with default bandwidth.

KEY RESOURCES TABLE

Reagent or Resource	Source	Identifier
Biological Samples		
Physa acuta snails, collected in the Lyon (France) population, and their descendants	This study	NA
Physa acuta snails, albino laboratory stock	[47]	NA
Critical commercial assays		
Short Read Eliminator Kit	Circulomics	#SS-100-101-01
TruSeq™ RNA Sample Prep Kit	Illumina	RS-122-2001
NEBNext Ultra II RNA Preparation Kit	New England Biolabs inc.	#E7775
Qiagen Blood & Cell Culture DNA Kit	Qiagen	#13323
Deposited Data		
Raw sequence reads, 21 transcriptomes of *Physa acuta*	This study	**https://www.ncbi.nlm.nih.gov/bioproject/PRJEB50799**
MinIon Raw sequences of *Physa acuta*, genomic DNA	This study	**https://www.ncbi.nlm.nih.gov/bioproject/PRJEB50799**
Sanger sequences of 30 *Physa acuta*, COI	This study	**https://www.ncbi.nlm.nih.gov/genbank** accessions OM667356 - OM667389
Sanger sequences of 30 *Physa acuta*, 16S	This study	**https://www.ncbi.nlm.nih.gov/genbank** accessions OM666692 - OM666725
Sanger sequences of 30 *Physa acuta*, 28S	This study	**https://www.ncbi.nlm.nih.gov/genbank** accessions OM666658 - OM666691
Oligonucleotides		
COI-F: GGTCAACAAATCATAAAGATATTGG	[50]	N/A
COI-R: TAAACTTCAGGGTGACCAAAAAATCA	[50]	N/A
16S-F: CGCCTGTTTAACAAAAACAT	This study	N/A
16S-R: CCGGTCTGAACTCAGATCACGT	This study	N/A
28S-F: ACCCGCTGAATTTAAGCAT	This study	N/A
28S-R: TCCGTGTTTCAAGACGGG	This study	N/A
D-specific internal primer for COI amplification, COI-FD: GGGACAACTAGGGTCTTAACTAC	This study	N/A
N-specific internal primer for COI amplification, COI-FN: GGAACATCTCTTGTACTRTTGGA	This study	N/A

Softwares and algorithms		
ape (v5.0)	[62]	**http://ape-package.ird.fr**
BLASTP (accessed november 2020)	[58]	**https://ftp.ncbi.nlm.nih.gov/blast**
ea-utils (v1.04.807)	[55]	**https://expressionanalysis.github.io/ea-utils**
FigTree (v1.4.2)	[68]	**https://github.com/rambaut/figtree/releases**
Flye (v2.8.1)	[65]	**https://github.com/fenderglass/Flye**
ggplot2 (v3.3.5)	[48]	**https://cran.r-project.org/web/packages/ggplot2**
Hierfstat (v0.5.7)	[53]	**https://cran.r-project.org/web/packages/hierfstat**
IMAGEJ (v1.52o)	[80]	**https://imagej.nih.gov**
lme4 (v1.1-21)	[71]	**https://cran.r-project.org/web/packages/lme4**
mapNH (in Bppml v2.2.0)	[70]	**https://github.com/BioPP/bppsuite**
MITObim (v1.6)	[63]	**https://github.com/chrishah/MITObim**
MITOS webserver	[64]	**http://mitos.bioinf.uni-leipzig.de**
phangorn (v2.4.0)	[61]	**https://cran.r-project.org/web/packages/phangorn**
Phylobayes (v3.3)	[49]	**http://www.atgc-montpellier.fr/phylobayes**
Prank (v170427)	[60]	**https://www.ebi.ac.uk/research/goldman/software/prank**
SeqinR (v4-2.4)	[66]	**https://seqinr.r-forge.r-project.org**
SiLiX (v1.2.11)	[59]	**https://help.rc.ufl.edu/doc/SiLiX**
STRUCTURE (v2.3.4)	[54]	**https://web.stanford.edu/group/pritchardlab/software/structure.html**
TransDecoder (v5.0.2)	N/A	**http://transdecoder.github.io**
Trinity (v2013-02-25)	[56]	**https://github.com/trinityrnaseq**
Bppml (v2.2.0)	[69]	**https://github.com/BioPP/bppsuite**

REFERENCES

1. Cosmides, L. M. and Tooby, J. (1981) Cytoplasmic inheritance and intragenomic conflict. J. Theor. Biol *89*, 83-129 .
2. Chase, C. D. (2007) Cytoplasmic male sterility: a window to the world of plant mitochondrial--nuclear interactions. Trends Genet. *23*, 81–90 .
3. Delph, L. F., Touzet, P. and Bailey, M. F. (2007). Merging theory and mechanism in studies of gynodioecy. Trends Ecol. Evol. *22*, 17–24.
4. Barrett, S. C. H. (2010). Darwin's legacy: the forms, function and sexual diversity of flowers. Philos. Trans. R. Soc. London B Biol. Sci. *365*, 351–368.
5. Dunn, D. F. (1975). Gynodioecy in an animal. Nature *253*, 528–529.
6. Weeks, S. C. (2012) The role of androdioecy and gynodioecy in mediating evolutionary transitions between dioecy and hermaphroditism in the Animalia. Evolution *66*, 3670–3686.
7. Vellnow, N., Vizoso, D. B., Viktorin, G. and Schärer, L. (2017). No evidence for strong cytonuclear conflict over sex allocation in a simultaneously hermaphroditic flatworm. BMC Evol. Biol. *17*, 103
8. J. C. Havird, Forsythe, E. S., Williams, A. M., Werren, J. H., Dowling, D. K., and Sloan, D. B. (2019). Selfish Mitonuclear Conflict. Curr. Biol. *29* R496–R511 .
9. Cho, Y., Mower, J. P., Qiu, Y.-L. and Palmer, J. D. (2004). Mitochondrial substitution rates are extraordinarily elevated and variable in a genus of flowering plants. Proc. Natl. Acad. Sci. U. S. A. *101*, 17741–17746 .
10. Mower, J. P., Touzet, P., Gummow, J. S., Delph, L. F. and Palmer, J. D. (2007). Extensive variation in synonymous substitution rates in mitochondrial genes of seed plants. BMC Evol. Biol. *7*, 135.
11. Touzet, P. and Budar, F. (2004). Unveiling the molecular arms race between two conflicting genomes in cytoplasmic male sterility? Trends Plant Sci. *9*, 568–570.
12. Fujii, S., Bond, C. S. and Small, I. D. (2011). Selection patterns on restorer-like genes reveal a conflict between nuclear and mitochondrial genomes throughout angiosperm evolution. Proc. Natl. Acad. Sci. U.S.A. *108*, 1723-1728.
13. Zimorski, V., Ku, C., Martin, W. F. and Gould, S. B. (2014). Endosymbiotic theory for organelle origins. Curr. Opin. Microbiol. *22*, 38–48.
14. Frank, S. A. and Hurst, L. D. (1996). Mitochondria and male disease. Nature *383*, 224
15. Gemmell, N. J., Metcalf, V. J. and Allendorf, F. W. (2004). Mother's curse: the effect of mtDNA on individual fitness and population viability. Trends Ecol. Evol. *19*, 238–244
16. Innocenti, P., Morrow, E. H. and Dowling, D. K. (2011). Experimental evidence supports a sex-specific selective sieve in mitochondrial genome evolution. Science *332*, 845–848
17. Perlman, S. J., Hodson, C. N., Hamilton, P. T., Opit, G. P. and Gowen, B. E. (2015). Maternal transmission, sex ratio distortion, and mitochondria. Proc. Natl. Acad. Sci. U.S.A. *112*, 10162–10168
18. Galtier, N. (2011).The intriguing evolutionary dynamics of plant mitochondrial DNA. BMC Biol. *9*, 61
19. Touzet, P. and Meyer, E. H. (2014). Cytoplasmic male sterility and mitochondrial metabolism in plants. Mitochondrion *19*, 166–171 .
20. Boore, J. L. (1999). Animal mitochondrial genomes. Nucleic Acids Res. *27*, 1767–1780.
21. Schärer, L. (2009) Tests of sex allocation theory in simultaneously hermaphroditic animals. Evolution *63*, 1377–1405.
22. Feng, S. Yang, Q., Li, H., Song, F., Stejskal, V., Opit, G. P., Cai, W., Li, Z., and Shao,

R. (2018). The highly divergent mitochondrial genomes indicate that the booklouse, *Liposcelis bostrychophila* (Psocoptera: Liposcelididae) is a cryptic species. G3 Genes, Genomes, Genet. *8*, 1039–1047.
23. Ebbs, E. T., Loker, E. S. and Brant, S. V. (2018). Phylogeography and genetics of the globally invasive snail Physa acuta Draparnaud 1805, and its potential to serve as an intermediate host to larval digenetic trematodes. BMC Evol. Biol. *18*, 103.
24. Nolan, J. R., Bergthorsson, U. and Adema, C. M. (2014). Physella acuta: atypical mitochondrial gene order among panpulmonates (Gastropoda). J. Molluscan Stud. *80*, 388–399.
25. Metzger, M. J., Villalba, A,. Carballal, M. J., Iglesias, D., Sherry, J., Reinisch, C., Muttray, A. F., Baldwin, S. A., and Goff, S. P. (2016). Widespread transmission of independent cancer lineages within multiple bivalve species. Nature *534*, 705–709.
26. Zouros, E. (2013). Biparental inheritance through uniparental transmission: the doubly uniparental inheritance (DUI) of mitochondrial DNA. Evol. Biol. *40*, 1–31.
27. Paraense, W. L. and Pointier, J.-P. (2003). Physa acuta Draparnaud, 1805 (Gastropoda: Physidae): a study of topotypic specimens. Mem. Inst. Oswaldo Cruz *98*, 513–517.
28. Chen, Z., Zhao, N., Li, S., Grover, C. E., Nie, H., Wendel, J. F., and Hua, J. (2017). Plant Mitochondrial Genome Evolution and Cytoplasmic Male Sterility. CRC. Crit. Rev. Plant Sci. *36*, 55–69.
29. Sloan, D. B., Alverson, A. J., Chuckalovcak, J. P., Wu, M., McCauley, D. E., Palmer, J. D., and Taylor, D. R. (2012). Rapid evolution of enormous, multichromosomal genomes in flowering plant mitochondria with exceptionally high mutation rates. PLoS Biol. *10*, e1001241.
30. Choi, K., Weng, M.-L., Ruhlman, T. A. and Jansen, R. K. (2021). Extensive variation in nucleotide substitution rate and gene/intron loss in mitochondrial genomes of Pelargonium. Mol. Phylogenet. Evol. *106986.*
31. Sloan, D. B., Müller, K., McCauley, D. E., Taylor, D. R. and Štorchová, H. (2012). Intraspecific variation in mitochondrial genome sequence, structure, and gene content in Silene vulgaris, an angiosperm with pervasive cytoplasmic male sterility. New Phytol. *196*, 1228–1239.
32. Darracq, A., Varré, J.-S., Maréchal-Drouard, L., Courseaux, A., Castric, V., Saumitou-Laprade, P., Oztas, S., Lenoble, P., Vacherie, B., Barbe, V. *et al.* (2011). Structural and content diversity of mitochondrial genome in beet: a comparative genomic analysis. Genome Biol. Evol. *3*, 723–736.
33. Bergero, R., Levsen, N., Wolff, K. and Charlesworth, D. (2019). Arms races with mitochondrial genome soft sweeps in a gynodioecious plant, Plantago lanceolata. Mol. Ecol. *28*, 2772–2785.
34. Patel, M. R., Miriyala, G. K., Littleton, A. J., Yang, H., Trinh, K., Young, J. M., Kennedy, S. R.,Yamashita, Y. M., Pallanck, L. J., Malik, H. S. (2016). A mitochondrial DNA hypomorph of cytochrome oxidase specifically impairs male fertility in Drosophila melanogaster. Elife *5*, e16923.
35. Camus, M. F. and Dowling, D. K. (2018).Mitochondrial genetic effects on reproductive success: signatures of positive intrasexual, but negative intersexual pleiotropy. Proc. R. Soc. B Biol. Sci. *285*, 20180187.
36. Chou, J.-Y. and Leu, J.-Y. (2015). The Red Queen in mitochondria: cyto-nuclear co-evolution, hybrid breakdown and human disease. Front. Genet. *6*, 187.
37. Hamilton, P. T., Hodson, C. N., Curtis, C. I. and Perlman, S. J. (2018). Genetics and genomics of an unusual selfish sex ratio distortion in an insect. Curr. Biol. *28*, 3864–3870.
38. Charlesworth, B. and Charlesworth, D. (1978). A model for the evolution of dioecy and

gynodioecy. Am. Nat. *112*, 975–997.
39. Jarne, P., Perdieu, M.-A., Pernot, A.-F., Delay, B. and David, P. (2000). The influence of self-fertilization and grouping on fitness attributes in the freshwater snail Physa acuta: Population and individual inbreeding depression. J. Evol. Biol. *13*, 645–655.
40. Dufay, M. and Billard, E. (2011). How much better are females? The occurrence of female advantage, its proximal causes and its variation within and among gynodioecious species. Ann. Bot. *109*, 505–519.
41. Thomaz, D., Guiller, A. and Clarke, B. (1996). Extreme divergence of mitochondrial DNA within species of pulmonate land snails. Proc. Roy. Soc. B. Biol. Sci. *263*, 363–368.
42. Giska, I., Sechi, P. and Babik, W. (2015). Deeply divergent sympatric mitochondrial lineages of the earthworm Lumbricus rubellus are not reproductively isolated. BMC Evol. Biol. *15*, 1–13.
43. Marletaz, F., Le Parco, Y., Liu, S. and Peijnenburg, K. T. C. A. (2017). Extreme Mitogenomic variation in natural populations of Chaetognaths. Genome Biol. Evol. *9*, 1374–1384.
44. Medina, M., Lal, S.,Vallès, Y., Takaoka, T. L., Dayrat, B. A., Boore, J. L., and Gosliner, T. (2011). Crawling through time: transition of snails to slugs dating back to the Paleozoic, based on mitochondrial phylogenomics. Mar. Genomics *4*, 51–59.
45. Dayrat, B., Conrad, M., Balayan, S., White, T. R., Albrecht, C., Golding, R., Gomes, S. R., Harasewych, M. G., and de Frias Martins, A.M. (2011).Phylogenetic relationships and evolution of pulmonate gastropods (Mollusca): new insights from increased taxon sampling. Mol. Phylogenet. Evol. *59*, 425–437.
46. Gray, J. (1988).Evolution of the freshwater ecosystem: the fossil record. Palaeogeogr. Palaeoclimatol. Palaeoecol. *62*, 1–214.
47. Noël, E., Chemtob, Y., Janicke, T., Sarda, V., Pélissié, B., Jarne, and David, P. (2016). Reduced mate availability leads to evolution of self-fertilization and purging of inbreeding depression in a hermaphrodite. Evolution *70*, 625–640.
48. Wickham, H. (2011). ggplot2. Wiley Interdiscip. Rev. Comput. Stat. *3*, 180–185.
49. Lartillot, N., Lepage, T. and Blanquart, S. (2009). PhyloBayes 3: A Bayesian software package for phylogenetic reconstruction and molecular dating. Bioinformatics *25*, 2286–2288.
50. Folmer, O., Black, M., Hoeh, W., Lutz, R. and Vrijenhoek, R. (1994). DNA primers for amplification of mitochondrial cytochrome c oxidase subunit I from diverse metazoan invertebrates. Mol. Mar. Biol. Biotechnol. *3*, 294–299.
51. Monsutti, A. and Perrin, N. (1999). Dinucleotide microsatellite loci reveal a high selfing rate in the freshwater snail Physa acuta. Mol. Ecol. *8*, 1076–1078.
52. Sourrouille, P., Debain, C. and Jarne, P. (2003). Microsatellite variation in the freshwater snail Physa acuta. Mol. Ecol. Notes *3*, 21–23.
53. Goudet, J. (2005). Hierfstat, a package for R to compute and test hierarchical F-statistics. Mol. Ecol. Notes *5*, 184–186.
54. Pritchard, J. K., Stephens, M. and Donnelly, P. (2000). Inference of population structure using multilocus genotype data. Genetics *155*, 945–959.
55. Aronesty, E. (2013). Comparison of sequencing utility programs. Open Bioinformatics J. *7*, 1-8
56. Grabherr, M. G., Haas, B. J., Yassour, M., Levin, J. Z., Thompson, D. A., Amit, I., Adiconis X., Fan, L., Raychowdhury, R., Zeng, Q. *et al.* (2011). Trinity: reconstructing a full-length transcriptome without a genome from RNA-Seq data. Nat. Biotechnol. *29*, 644-652.
57. Burgarella, C., Gayral, P., Ballenghien, M., Bernard, A., David, P., Jarne, P., Correa,

A., Hurtrez-Bousses, S., Escobar, J., Galtier, N. *et al.* (2015). Molecular evolution of freshwater snails with contrasting mating systems. Mol. Biol. Evol. **32**, 2403-2416.
58. Altschul, S. F., Gish, W., Miller, W., Myers, E. W. and Lipman, D. J. (1990). Basic local alignment search tool. J. Mol. Biol. *215*, 403–410.
59. Miele, V., Penel, S. and Duret, L. (2011). Ultra-fast sequence clustering from similarity networks with SiLiX. BMC Bioinformatics *12*, 1–9.
60. Loytynoja, A. and Goldman, N.(2005). From The Cover: An algorithm for progressive multiple alignment of sequences with insertions. Proc. Natl. Acad. Sci. U.S.A. *102*, 10557–10562.
61. Schliep, K. P. phangorn: phylogenetic analysis in R. (2011). Bioinformatics *27*, 592–593.
62. Paradis, E., Claude, J. and Strimmer, K. (2004). APE: analyses of phylogenetics and evolution in R language. Bioinformatics *20*, 289–290.
63. Hahn, C., Bachmann, L. and Chevreux, B. (2013). Reconstructing mitochondrial genomes directly from genomic next-generation sequencing reads—a baiting and iterative mapping approach. Nucleic Acids Res. *41*, e129-e129.
64. Bernt, M., Donath, A., Jühling, F., Externbrink, F., Florentz, C., Fritzsch, G., Pütz, J., Middendorf, M., and Stadler, P. (2013). MITOS: improved de novo metazoan mitochondrial genome annotation. Mol. Phylogenet. Evol. *69*, 313–319.
65. Kolmogorov, M., Yuan, J., Lin, Y. and Pevzner, P. A. (2019). Assembly of long, error-prone reads using repeat graphs. Nat. Biotechnol. *37*, 540–546.
66. Charif, D. and Lobry, J. R. (2007) SeqinR 1.0-2: a contributed package to the R project for statistical computing devoted to biological sequences retrieval and analysis. In Structural Approaches To Sequence Evolution*,* Bastolla, U., Porto, M., Roman, H. E., and Vendruscolo, M., eds. (Berlin: Springer), pp. 207–232.
67. Castresana, J. (2000). Selection of conserved blocks from multiple alignments for their use in phylogenetic analysis. Mol. Biol. Evol. *17*, 540–552.
68. Rambaut, A. and Drummond, A. J. (2012). FigTree. Version 1.4. 0. Available at *http/tree.bio.ed.ac.uk/software/figtree.*
69. Guéguen, L. Gaillard, S., Boussau, B., Gouy, M., Groussin, M., Rochette, N. C., Bigot, T., Fournier, D., Pouyet, F., Cahais, V. *et al.* (2013). Bio++: Efficient Extensible Libraries and Tools for Computational Molecular Evolution. Mol. Biol. Evol. *30*, 1745–1750.
70. Guéguen, L. and Duret, L. (2017).Unbiased Estimate of Synonymous and Nonsynonymous Substitution Rates with Nonstationary Base Composition. Mol. Biol. Evol. *35*, 734–742.
71. Bates, D., Mächler, M., Bolker, B. and Walker, S. (2014).Fitting linear mixed-effects models using lme4. arXiv*1406.5823.*
72. Janicke, T., Vellnow, N., Sarda, V. and David, P. (2013). Sex-Specific inbreeding depression depends on the strength of male-male competition. Evolution *67*, 2861–2875
73. Bonel, N., Noël, E., Janicke, T., Sartori, K., Chapuis, E., Ségard, A., Meconcelli, S., Pélissié, B., Sarda, V., and David, P. (2018).Asymmetric evolutionary responses to sex-specific selection in a hermaphrodite. Evolution*. 72*, 2181–2201.
74. Pélissié, B., Jarne, P., and David, P. (2012). Sexual selection without sexual dimorphism: Bateman gradients in a simultaneous hermaphrodite. Evolution*. 66*, 66–81.
75. Noël, E., Jarne, P., Glémin, S., MacKenzie, A., Segard, A., Sarda, V., and David, P. (2017). Experimental Evidence for the Negative Effects of Self-Fertilization on the Adaptive Potential of Populations. Curr. Biol. *27*, 237–242.

76. Tsitrone, A., Jarne, P., and David, P. (2003). Delayed selfing and resource reallocations in relation to mate availability in the freshwater snail Physa acuta. Am. Nat. *162*, 474–488.
77. Escobar, J. S., Facon, B., Jarne, P., Goudet, J., and David, P. (2009). Correlated evolution of mating strategy and inbreeding depression within and among populations of the hermaphroditic snail physa acuta. Evolution. *63***,** 2790-2804.
78. Jarne, P., Perdieu, M.-A. Pernot, A.-F. Delay, B., and David, P. (2000). The influence of self-fertilization and grouping on fitness attributes in the freshwater snail Physa acuta: Population and individual inbreeding depression. J. Evol. Biol. *13*, 645–655.
79. Escobar, J. S., Nicot, A., and David, P. (2008). The different sources of variation in inbreeding depression, heterosis and outbreeding depression in a metapopulation of Physa acuta. Genetics *180*, 1593–1608.
80. Schneider, C. A., Rasband, W. S. and Eliceiri, K. W. (2012). NIH Image to ImageJ: 25 years of image analysis. Nat. Methods *9*, 671–675.

David et al. 2022

Supplementary figures and tables

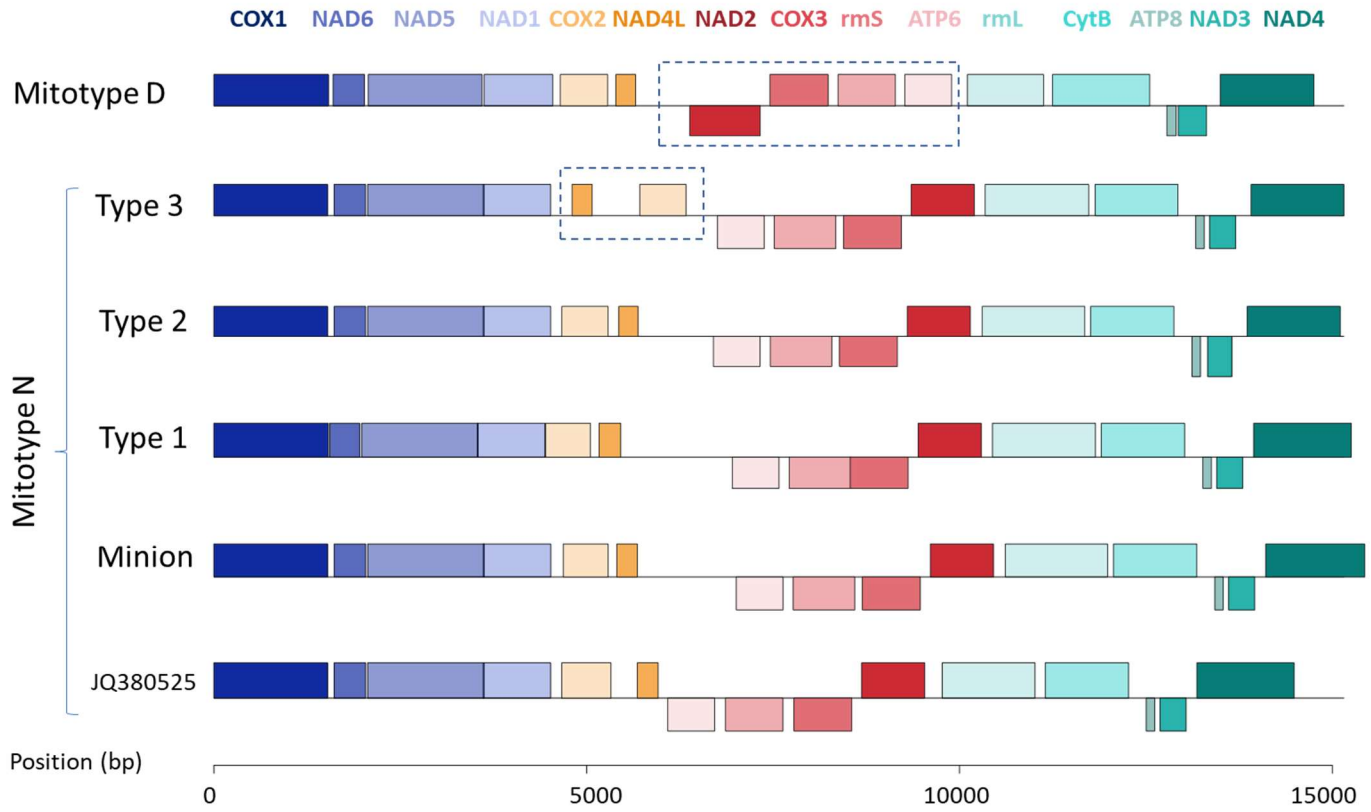

Figure S1. Structural variants in the assembled mitogenomes of D and N individuals of *P. acuta.* Related to Figure 1. Gene orders are displayed for 20 reassembled mtDNA sequences from transcriptomes of the Lyon population, falling into four structural variants: one for the D mitotype (10 individuals) and three for the N mitotype (4, 3 and 3 individuals of type 1, 2 and 3 respectively). We also represent the mtDNA of another N individual collected in a natural population near Lyon (see Methods) obtained from a MinION long-fragment sequencer ("Minion") – its similarity with other N individuals rules out any strong bias specific to transciptome-based assembly. The JQ380525 sample (referred by its Genbank accession number) is isolate A from New Mexico (USA[S1]) and is also of mitotype N. For easier reading, the mitogenomes are represented in linear form, tRNA genes are omitted, boxes are represented above or below the line depending on whether the coding sequence is on the "+" or "-" strand, and zones with changes in gene order, compared to the JQ380525 reference, are framed in a blue dotted line. The details of annotations are represented in Table S1.

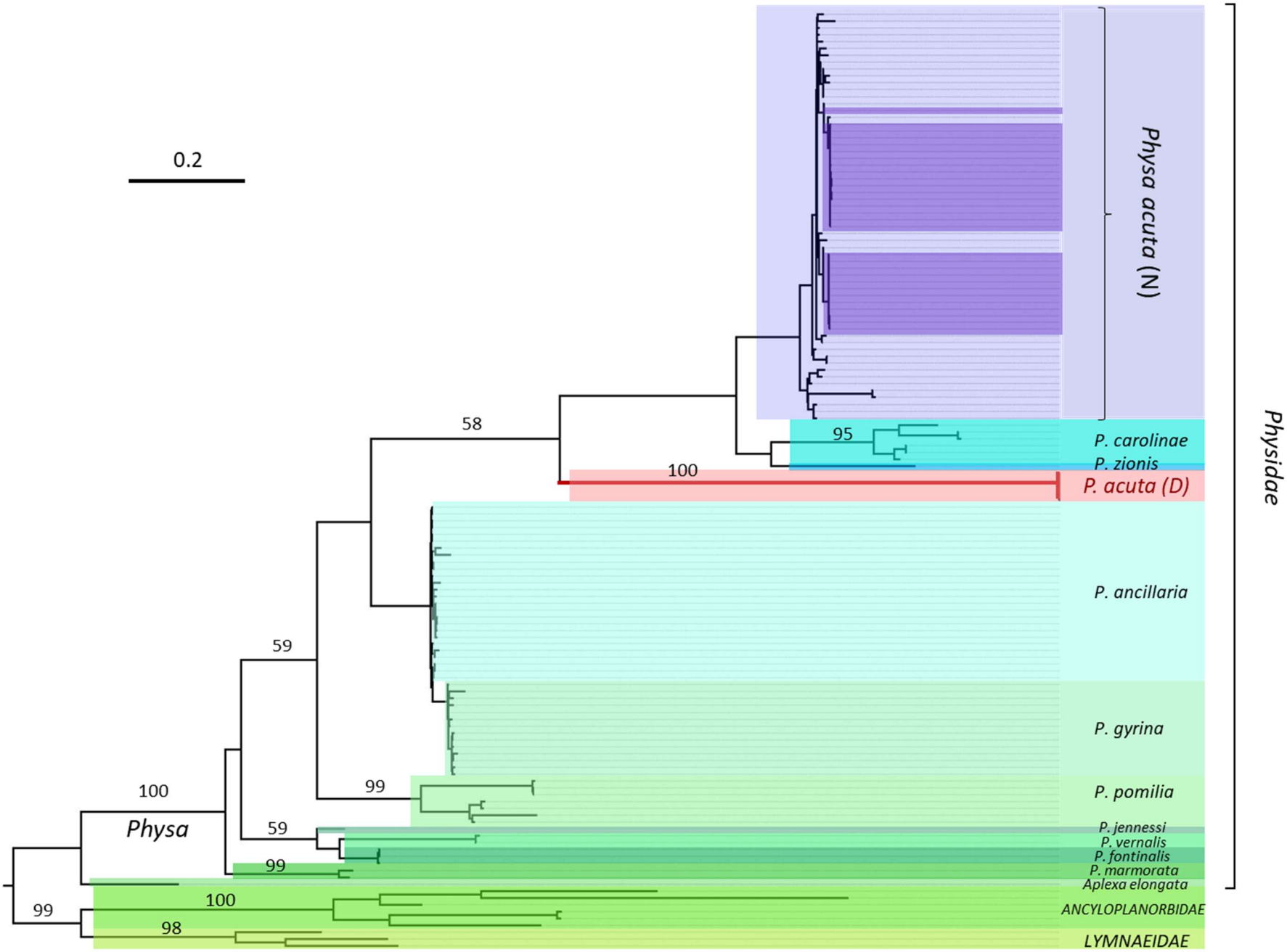
0.2
Physa acuta (N)
Physidae
58
95
P. carolinae
P. zionis
100
P. acuta (D)
P. ancillaria
59
P. gyrina
100
99
P. pomilia
Physa
59
P. jennessi
P. vernalis
P. fontinalis
P. marmorata
99
Aplexa elongata
100
ANCYLOPLANORBIDAE
99
98
LYMNAEIDAE

Figure S2. Position of the divergent D mitotype of *P. acuta* within the Physidae phylogeny (based on 137 concatenated mitochondrial COI and 16S sequences). Related to Figure 1. The very long branch (in red) leading to D sequences makes the exact branching point uncertain (in phylogenetic reconstruction, long branches tend to be attracted to each other). However, the origin of the D branch is definitely within the genus *Physa*. The phylogeny was obtained using *Phylobayes* using the CAT-GTR+G+I model. The Ancyloplanorbidae and Lymnaeidae have been used as outgroups. Bayesian posterior probabilities (in %) are indicated at species-level and deeper nodes, only when they were >50%. All haplotypes of *P. acuta* other than the D lineage are collectively called "N". All sequences of *P. acuta* D, as well as the sequences of *P. acuta* N highlighted in deep purple, were obtained from the present study (individuals from the Lyon population, France). Other sequences were retrieved from GenBank (accessions in Data S1C). Note that the taxonomy of *P. acuta* and allies (as for many freshwater snails) has been historically burdened by an abundance of dubious species names. Here the delimitation of *P. acuta* follows the taxonomic revision in refs [S2–S4] who synonymized several names under *P. acuta* based on tests of interbreeding ability in the laboratory. Samples named *P. spelunca* branch within the *P. acuta* clade, so this taxon has also been considered a synonym of *P. acuta* (otherwise the set of interbreeding populations *P. acuta* would be paraphyletic), although interbreeding was never tested. The status of *P. zionis* as distinct from *P. acuta* has not been checked by interbreeding tests, and is still open to question, while the sister clade *P. carolinae* is reproductively isolated from *P. acuta*[S4]. Similarly, we adopted a broad definition of "Physa" as a monophyletic genus and did not use genus names (*Haitia, Physella, Petrophysa*) that lead to paraphyly.

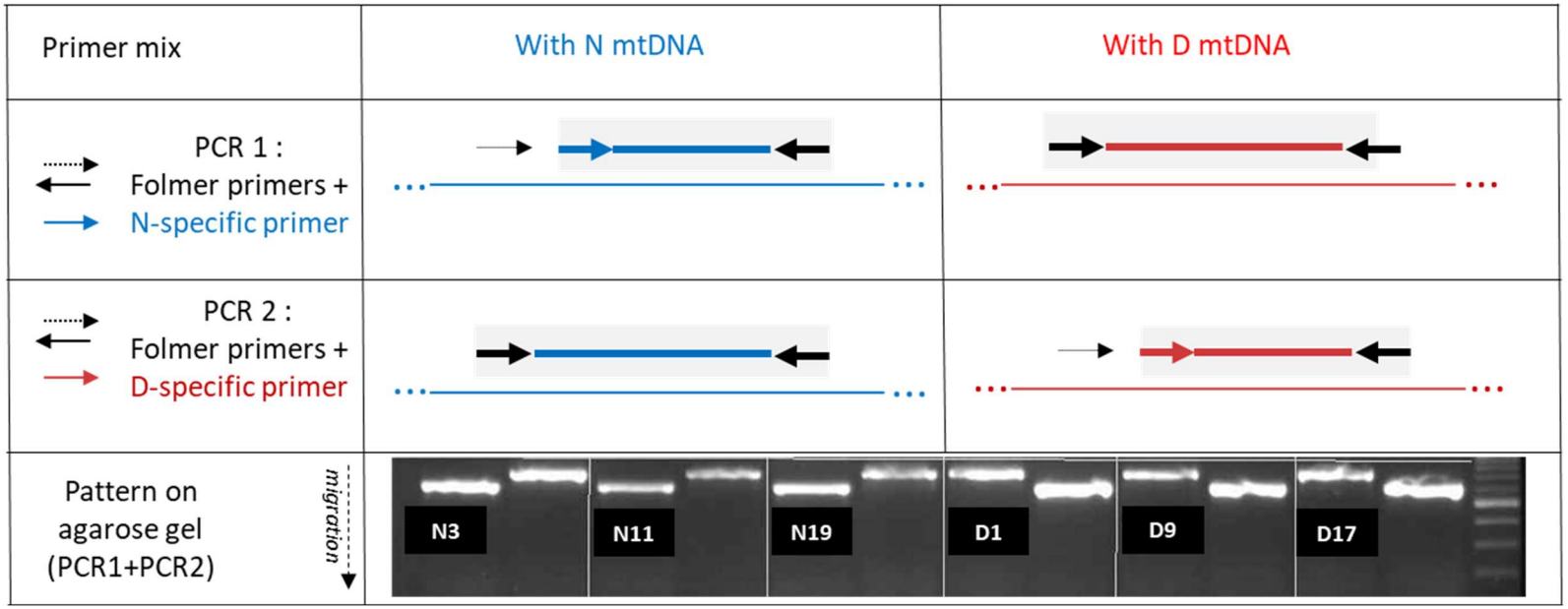

Figure S3. Mitotype identification by PCR. Related to STAR Methods. Two PCRs were performed per individual using three primers per PCR, the two external, universal COI "Folmer" primers (black; sequences in Key resources Table) and one of two internal specific primers (GGAACATCTCTTGTACTRTTGGA for N and GGGACAACTAGGGTCTTAACTAC for D mitotypes, blue and red respectively). Each internal primer blocks the amplification of the long fragment in its specific mitotype. PCR products were run side by side on an agarose gel (2%), giving a typical pattern of short-long (N) or long-short (D) fragments (an example of gel with individuals from three maternal lines of each mitotype is given). Short and long fragments span 604 and 705 bp respectively. Amplifications were carried out in 20 µL reaction volume comprising 2 µL 10X standard buffer (Eurobio), 0.17 µL dNTP mix (20mM), 0.4 µL of each primer (10µM), 0.2 µL 100X BSA, 0.6 µL 50mM MgCl2, 0.17 µL EurobioTaq DNA polymerase (5U/µL, Eurobio) and 2µL DNA extract. The PCR conditions were as follows: 5 min at 94 ˚C, followed by 40 cycles of denaturation for 30 s at 94 ˚C, annealing for 30 s at 50 ˚C and extension for 40 s at 72 ˚C completed with a final extension (72 ˚C, 18 min).

	Physa JQ390525		Physa N MinION		Physa N T1 (ind. N35)		Physa N T2 (ind. N27)		Physa N T3 (ind. N31)		Physa D (ind. W1)	
	START	STOP	START	STOP	START	STOP	START	STOP	START	STOP	START	STOP
cox1	1	1527	1	1527	1	1536	1	1527	1	1527	1	1527
trnP(cca)	1552	1614	1552	1614	NA	NA	1551	1613	1553	1613	1552	1614
nad6	1616	2038	1616	2038	1554	1958	1615	2037	1615	2037	1616	2038
nad5	2064	3626	2064	3626	1984	3546	2063	3625	2063	3625	2064	3626
nad1	3614	4519	3614	4519	3534	4439	3613	4518	3613	4518	3614	4519
trnD(gac)	4523	4590	4523	4590	NA	NA	4522	4589	4522	4588	4523	4590
trnF(ttc)	4603	4667	4603	4667	NA	NA	4602	4666	4601	4665	4603	4667
cox2	4687	5289	4687	5289	4449	5051	4668	5288	5713	6333	4687	5289
trnW(tga)	5405	5680	5338	5403	5100	5165	5347	5412	4736	4803	5405	5680
nad4l	5757	5821	5405	5680	5167	5457	5432	5689	4805	5074	5757	5821
trnY(tac)	5338	5403	5757	5821	5691	5755	6448	6512	6358	6422	5338	5403
trnS1(aga)	NA	NA	5816	5882	5750	5816	NA	NA	NA	NA	NA	NA
trnM(atg)	7706	7777	6031	6096	5859	5921	8242	8307	8296	8361	7706	7777
trnC(tgc)	5816	5882	6421	6482	6302	6363	5688	5749	5647	5711	5816	5882
trnQ(caa)	6031	6096	6929	7002	6873	6946	6623	6696	6677	6750	9611	10456
atp6	6421	6482	7007	7633	6954	7580	6700	7326	6755	7381	9525	9598
trnR(cga)	6929	7002	7635	7701	7582	7648	7328	7394	7383	7449	8699	9475
trnE(gaa)	7007	7633	7706	7777	7653	7724	7399	7470	7454	7525	8624	8696
rrnS	7635	7701	7770	8596	7717	8560	7463	8288	7516	8342	7770	8596
trnT(aca)	7770	8596	8624	8696	5934	5983	8316	8388	8370	8443	7635	7701
cox3	8624	8696	8699	9475	8535	9311	8391	9167	8446	9222	7007	7633
trnI(atc)	8699	9475	9525	9598	9361	9434	9214	9287	9269	9341	6929	7002
nad2	9525	9598	9611	10456	9447	10292	9300	10145	9354	10199	6421	6482
trnK(aaa)	9611	10456	10486	10555	10322	10391	10179	10231	10226	10289	6031	6096
trnV(gta)	10486	10555	10612	10686	NA	NA	10301	10375	NA	NA	10486	10555
rrnL	10612	10686	10615	11987	10443	11824	10304	11680	10345	11733	10612	10686
trnL1(cta)	10615	11987	11934	11989	11771	11826	11627	11682	11680	11735	10615	11987
trnA(gca)	11934	11989	11990	12063	11827	11900	11683	11756	11736	11809	11934	11989
cob	11990	12063	12065	13183	11902	13020	11758	12876	11819	12929	11990	12063
trnG(gga)	12065	13183	13197	13249	13034	13088	12890	12942	12943	12994	12065	13183
trnH(cac)	13197	13249	13250	13312	13089	13151	12943	13005	12995	13056	13197	13249
trnL2(tta)	13250	13312	13315	13379	13154	13218	13008	13073	13059	13123	13250	13312
atp8	13315	13379	13425	13538	13265	13378	13119	13232	13169	13282	13315	13379
trnN(aac)	13425	13538	13540	13606	13380	13446	13234	13300	13284	13350	13425	13538
nad3	13540	13606	13610	13960	13450	13800	13329	13654	13354	13704	13540	13606
trnS2(tca)	13610	13960	13964	14026	13804	13866	13658	13720	13719	13781	13610	13960
trnS1(agc)	13964	14026	14035	14095	13875	13935	13729	13788	13779	13838	13964	14026
nad4	14035	14095	14107	15435	13947	15254	13860	15106	13911	15155	14035	14095

Table S1. Positions of all annotated genes in the complete mitogenome sequences. Related to Figure 1 and Figure S1.

Gene	dS(D)	dS(D)/dS(N)	dN/dS (N)	dN/dS (D)	Kr/Kc (N)	Kr/Kc (D)
ATP6	7.824	4.54	0.033	0.04	0.897	0.734
COX1	7.682	4.657	0.006	0.025	0.313	0.601
COX2	7.617	3.931	0.067	0.046	1.021	0.677
COX3	7.832	4.746	0.027	0.052	1.036	0.827
CYTB	7.618	4.577	0.031	0.045	0.645	0.775
NAD1	7.685	4.118	0.063	0.049	0.653	0.772
NAD2	7.847	4.496	0.082	0.064	0.869	0.821
NAD3	7.783	4.301	0.072	0.05	0.483	1.07
NAD4	7.745	4.805	0.051	0.049	0.593	0.684
NAD5	7.873	4.55	0.072	0.055	0.788	0.879
NAD6	7.821	4.772	0.077	0.06	0.815	0.686
All	7.748	4.508	0.047	0.046	0.749	0.767

Table S2. **Substitution patterns in the D and N mitotypes**. **Related to Figure 1.** A phylogeny was made using an alignment of all 11 concatenated protein-coding genes available in the mtDNA. We included one individual of mitotype D (all D individuals had identical sequences), six individuals of mitotype N representative of the available diversity, and one outgroup (*P. gyrina*). The rates of synonymous (dS), nonsynonymous (dN), radical (Kr) and conservative (Kc) substitutions were estimated separately, under the YN98 codon model, for each gene, in two branches: the branch from the common ancestor of all *P. acuta* to the D mitotype, and the branch from the common ancestor to the N mitotype (in that case, estimates were averaged over the six individuals). "All" refers to estimates obtained using the concatenation of all 11 genes. dS(D) = estimated rate of synonymous substitutions in the D branch – values above 1 occur when several synonymous substitutions have taken place successively in the same site. dS(D)/dS(N) = estimated ratio of synonymous substitution rates between the D and N branches. dN/dS = ratio of nonsynonymous to synonymous substitutions (given for D and N branches separately). Kr/Kc, ratio of radical to conservative amino-acid substitutions (idem).

Supplemental References

S1. Nolan, J. R., Bergthorsson, U. and Adema, C. M. *Physella acuta*: atypical mitochondrial gene order among panpulmonates (Gastropoda). J. Molluscan Stud. *80*, 388–399.

S2. Wethington, A. R. and Lydeard, C. (2007). A molecular phylogeny of Physidae (Gastropoda: Basommatophora) based on mitochondrial DNA sequences. J. Molluscan Stud. *73*, 241–257.

S3. Dillon, R. T., Robinson, J. D. and Wethington, A. R. (2007). Empirical estimates of reproductive isolation among the freshwater pulmonate snails *Physa acuta*, *P. pomilia*, and *P. hendersoni*. Malacologia *49*, 283–292.

S4. Dillon, R. T., Wethington, A. R. and Lydeard, C. (2011). The evolution of reproductive isolation in a simultaneous hermaphrodite, the freshwater snail *Physa*. BMC Evol. Biol. *11*, 1–12.

LEGENDS FOR SUPPLEMENTARY DATA

Data S1. Accessions of mitochondrial sequences used in this study. Related to STAR Methods and Figure 1. A) Genbank accessions of mitochondrial Cytochrome oxydase subunit I (COI) sequences in various gastropods, used in combination with our own sequences of *P. acuta* from Lyon to generate Figure 1A. For each sample, taxonomic groupings are provided (from lower to higher: family, clade_2, clade-1, and subclass). The column "distance" refers to the different categories in figure 1a: 0 = *P. acuta*; 1 = other Physidae; 2 = other Hygrophila; 3 = other Panpulmonata; 4 = other Gastropods. **B)** Accessions of complete mtDNA sequences used in Figure 1B, in combination with our own sequences of *P. acuta* from Lyon**.** For each sample, taxonomical groupings are provided (from lower to higher: family, clade 2, clade 1). For *Physa gyrina*, we reassembled the mtDNA from the available transcriptome reads; the accession provided is that of the reads in the SRA database. **C)** GenBank accessions of COI and 16S sequences of Physidae and other Hygrophila, that were used, in conjunction with our own COI and 16S sequences of 34 *Physa acuta* from the Lyon population (5 of mitotype D+29 of mitotype N), to generate Figure S2. Because of taxonomical revisions posterior to submission to GenBank, our taxon names, indicated in the "Taxon (1)" column, sometimes differ from the original names in GenBank ("Taxon (2)"). All *Physa acuta* sequences in the three sections (A, B and C) belong to the N mitotype.

Data S2. Results of linear models on behavioral and fitness traits of *Physa acuta* N and D individuals. Related to STAR methods and Figure 3. A) Sexual behavior of N and D snails from Lyon paired with N partners from the albino reference population. **B)** Sexual behavior of N and D snails from Lyon paired with each other (*idem*). Only male traits are displayed (female traits of focals equal male traits of partner, so the female table would be identical, with partner and focal swapped). Effects of focal type and partner type are included, as well as their interaction (when significant, the partner type effect is tested within each focal type, and reciprocally). Note that an effect of mitotype on female behavior would result in an effect of partner type on male traits in this analysis. Thus, the significant interaction between own type and partner type on male time reflects the fact that, in pairs of nonvirgin snails, N individuals tend to spend less time acting as males with a N partner than they do with a D partner – suggesting that D individuals may be more attractive as females in some circumstances. **C)** fitness traits of N and D snails paired with partners from the albino reference population. Note that D snails paired with virgin albino often did not stimulate egg-laying in their partner, and most of the clutches laid by partners of D snails turned out to be self-fertilized (100% albino juveniles recovered, or 0% paternity rate for the focal individual). In contrast, egg production by nonvirgin albino mates was the same, irrespective of whether they were paired with D or N focal snails– this is because once inseminated, snails store sperm and are no longer dependent on sperm receipt to start laying eggs. Nonvirgin albino mates usually produced either 100% albino or mixed albino-pigmented progeny, reflecting sperm competition between the focal's allosperm and the previously stored "albino" allosperm. **D)** fitness traits of virgin N and D snails from Lyon paired with each other (in these monogamous pairs, female

fitness of one snail equals male fitness of the other). Note that most partners of D snails did not lay eggs at all, confirming that D snails failed to stimulate egg-laying in virgin snails of their own population, as they did with virgin albino snails. **E)** Fitness traits of isolated, virgin individuals (obligate self-fertilization). Note that individuals that died without reproducing were on average very old (age of death 132.5 ± 6.5 days in D, 110.8 ± 11.8 in N; sexual maturity is usually reached at 45-50 days). Note also that self-fertilization sterility in D snails was not total, as a few juveniles were finally produced by 14 of the 122 D individuals**. F)** Sperm production traits in virgin individuals. As D snails were significantly bigger than N snails in this experiment (body weight D: 139.5+/-4.2 mg versus N : 122.7 +/- 3.0 mg, χ^2=9.54, P=0.002), and body weight had a significant effect on the traits analysed, we kept body weight as a covariate in the models.

Throughout Data S2, traits highlighted in yellow are those represented in Figure 3 (main text). The "status" column refers to previous mating history of the individual ("virgin" for individuals encountering mates for the first time, "experienced" or "nonvirgin" otherwise). Performances of N and D mitotypes are reported either as trait means and SE (for quantitative traits) or as successes / failures (success = at least one copulation observed, or at least one egg or juvenile produced, failure = no copulation, egg or juvenile). Likelihood-ratio tests are reported for fixed effects (*P*-values < 0.05 are in bold characters). The last columns indicate the random effects included in the model and the distribution of the variable. Blue: male traits, red: female traits, purple: male and female traits (selfing individuals are both father and mother of their offspring).

SUPPLEMENTARY DATA

Accession	Genus	species	distance	Family	clade_2	clade_1	subclass
NC_023253	Physa	acuta	0	Physidae	Hygrophila	Panpulmonata	Heterobranchia
JQ390526	Physa	acuta	0	Physidae	Hygrophila	Panpulmonata	Heterobranchia
GU247996	Physa	acuta	0	Physidae	Hygrophila	Panpulmonata	Heterobranchia
GU247995	Physa	acuta	0	Physidae	Hygrophila	Panpulmonata	Heterobranchia
GU247993	Physa	acuta	0	Physidae	Hygrophila	Panpulmonata	Heterobranchia
AY651203	Physa	acuta	0	Physidae	Hygrophila	Panpulmonata	Heterobranchia
AY651193	Physa	acuta	0	Physidae	Hygrophila	Panpulmonata	Heterobranchia
AY651192	Physa	acuta	0	Physidae	Hygrophila	Panpulmonata	Heterobranchia
AY651188	Physa	acuta	0	Physidae	Hygrophila	Panpulmonata	Heterobranchia
AY651186	Physa	acuta	0	Physidae	Hygrophila	Panpulmonata	Heterobranchia
AY651185	Physa	acuta	0	Physidae	Hygrophila	Panpulmonata	Heterobranchia
AY651181	Physa	acuta	0	Physidae	Hygrophila	Panpulmonata	Heterobranchia
AY651174	Physa	acuta	0	Physidae	Hygrophila	Panpulmonata	Heterobranchia
AY651203	Physa	acuta	0	Physidae	Hygrophila	Panpulmonata	Heterobranchia
AY282589	Physa	acuta	0	Physidae	Hygrophila	Panpulmonata	Heterobranchia
EU038389	Physa	acuta	0	Physidae	Hygrophila	Panpulmonata	Heterobranchia
EU038372	Physa	acuta	0	Physidae	Hygrophila	Panpulmonata	Heterobranchia
EU038371	Physa	acuta	0	Physidae	Hygrophila	Panpulmonata	Heterobranchia
EU038368	Physa	acuta	0	Physidae	Hygrophila	Panpulmonata	Heterobranchia
EU038367	Physa	acuta	0	Physidae	Hygrophila	Panpulmonata	Heterobranchia
EU038366	Physa	acuta	0	Physidae	Hygrophila	Panpulmonata	Heterobranchia
EU038365	Physa	acuta	0	Physidae	Hygrophila	Panpulmonata	Heterobranchia
EU038361	Physa	acuta	0	Physidae	Hygrophila	Panpulmonata	Heterobranchia
EU038360	Physa	acuta	0	Physidae	Hygrophila	Panpulmonata	Heterobranchia
EU038357	Physa	acuta	0	Physidae	Hygrophila	Panpulmonata	Heterobranchia
EU038356	Physa	acuta	0	Physidae	Hygrophila	Panpulmonata	Heterobranchia
EU038355	Physa	acuta	0	Physidae	Hygrophila	Panpulmonata	Heterobranchia
KJ769128	Physa	acuta	0	Physidae	Hygrophila	Panpulmonata	Heterobranchia
KJ769127	Physa	acuta	0	Physidae	Hygrophila	Panpulmonata	Heterobranchia
KJ769126	Physa	acuta	0	Physidae	Hygrophila	Panpulmonata	Heterobranchia
KJ769125	Physa	acuta	0	Physidae	Hygrophila	Panpulmonata	Heterobranchia
KJ769124	Physa	acuta	0	Physidae	Hygrophila	Panpulmonata	Heterobranchia
KJ769123	Physa	acuta	0	Physidae	Hygrophila	Panpulmonata	Heterobranchia
JQ390526	Physa	acuta	0	Physidae	Hygrophila	Panpulmonata	Heterobranchia
JQ390525	Physa	acuta	0	Physidae	Hygrophila	Panpulmonata	Heterobranchia
KT280445	Physa	acuta	0	Physidae	Hygrophila	Panpulmonata	Heterobranchia
KT280444	Physa	acuta	0	Physidae	Hygrophila	Panpulmonata	Heterobranchia
KT280443	Physa	acuta	0	Physidae	Hygrophila	Panpulmonata	Heterobranchia
KT280442	Physa	acuta	0	Physidae	Hygrophila	Panpulmonata	Heterobranchia
KT280441	Physa	acuta	0	Physidae	Hygrophila	Panpulmonata	Heterobranchia
KT280440	Physa	acuta	0	Physidae	Hygrophila	Panpulmonata	Heterobranchia
KT280439	Physa	acuta	0	Physidae	Hygrophila	Panpulmonata	Heterobranchia
KT280438	Physa	acuta	0	Physidae	Hygrophila	Panpulmonata	Heterobranchia
KT280437	Physa	acuta	0	Physidae	Hygrophila	Panpulmonata	Heterobranchia
KT280436	Physa	acuta	0	Physidae	Hygrophila	Panpulmonata	Heterobranchia
KT280435	Physa	acuta	0	Physidae	Hygrophila	Panpulmonata	Heterobranchia
AY651184	Physa	acuta	0	Physidae	Hygrophila	Panpulmonata	Heterobranchia
AY651183	Physa	acuta	0	Physidae	Hygrophila	Panpulmonata	Heterobranchia
AY651177	Physa	acuta	0	Physidae	Hygrophila	Panpulmonata	Heterobranchia
AY651176	Physa	acuta	0	Physidae	Hygrophila	Panpulmonata	Heterobranchia
AY651171	Physa	acuta	0	Physidae	Hygrophila	Panpulmonata	Heterobranchia
AY651170	Physa	acuta	0	Physidae	Hygrophila	Panpulmonata	Heterobranchia
AY651198	Physa	zionis	1	Physidae	Hygrophila	Panpulmonata	Heterobranchia
EU038396	Physa	sp_A	1	Physidae	Hygrophila	Panpulmonata	Heterobranchia
EU038395	Physa	sp_A	1	Physidae	Hygrophila	Panpulmonata	Heterobranchia
EU038392	Physa	ancillaria	1	Physidae	Hygrophila	Panpulmonata	Heterobranchia
EU038391	Physa	ancillaria	1	Physidae	Hygrophila	Panpulmonata	Heterobranchia
EU038387	Physa	ancillaria	1	Physidae	Hygrophila	Panpulmonata	Heterobranchia
EU038386	Physa	ancillaria	1	Physidae	Hygrophila	Panpulmonata	Heterobranchia
EU038385	Physa	ancillaria	1	Physidae	Hygrophila	Panpulmonata	Heterobranchia
EU038384	Physa	ancillaria	1	Physidae	Hygrophila	Panpulmonata	Heterobranchia
EU038383	Physa	ancillaria	1	Physidae	Hygrophila	Panpulmonata	Heterobranchia
EU038382	Physa	ancillaria	1	Physidae	Hygrophila	Panpulmonata	Heterobranchia
EU038380	Physa	ancillaria	1	Physidae	Hygrophila	Panpulmonata	Heterobranchia
EU038379	Physa	ancillaria	1	Physidae	Hygrophila	Panpulmonata	Heterobranchia
EU038378	Physa	ancillaria	1	Physidae	Hygrophila	Panpulmonata	Heterobranchia

EU038359	Physa	ancillaria	1	Physidae	Hygrophila	Panpulmonata	Heterobranchia
EU038358	Physa	ancillaria	1	Physidae	Hygrophila	Panpulmonata	Heterobranchia
EU038377	Physa(Aplexa)	elongata	1	Physidae	Hygrophila	Panpulmonata	Heterobranchia
EU038375	Physa(Aplexa)	elongata	1	Physidae	Hygrophila	Panpulmonata	Heterobranchia
EU038363	Physa	pomilia	1	Physidae	Hygrophila	Panpulmonata	Heterobranchia
EU038354	Physa	pomilia	1	Physidae	Hygrophila	Panpulmonata	Heterobranchia
EU038353	Physa	pomilia	1	Physidae	Hygrophila	Panpulmonata	Heterobranchia
AY651196	Physa	hendersoni	1	Physidae	Hygrophila	Panpulmonata	Heterobranchia
AY651195	Physa	hendersoni	1	Physidae	Hygrophila	Panpulmonata	Heterobranchia
AY651194	Physa	hendersoni	1	Physidae	Hygrophila	Panpulmonata	Heterobranchia
EU038398	Physa	gyrina	1	Physidae	Hygrophila	Panpulmonata	Heterobranchia
EU038374	Physa	gyrina	1	Physidae	Hygrophila	Panpulmonata	Heterobranchia
EU038373	Physa	gyrina	1	Physidae	Hygrophila	Panpulmonata	Heterobranchia
AY651200	Physa	gyrina	1	Physidae	Hygrophila	Panpulmonata	Heterobranchia
AY651199	Physa	gyrina	1	Physidae	Hygrophila	Panpulmonata	Heterobranchia
AY651197	Physa	gyrina	1	Physidae	Hygrophila	Panpulmonata	Heterobranchia
AY651191	Physa	gyrina	1	Physidae	Hygrophila	Panpulmonata	Heterobranchia
AY651187	Physa	gyrina	1	Physidae	Hygrophila	Panpulmonata	Heterobranchia
AY651182	Physa	gyrina	1	Physidae	Hygrophila	Panpulmonata	Heterobranchia
AY651178	Physa	gyrina	1	Physidae	Hygrophila	Panpulmonata	Heterobranchia
AY651173	Physa	gyrina	1	Physidae	Hygrophila	Panpulmonata	Heterobranchia
AY651172	Physa	gyrina	1	Physidae	Hygrophila	Panpulmonata	Heterobranchia
EU038369	Physa(Aplexa)	marmorata	1	Physidae	Hygrophila	Panpulmonata	Heterobranchia
EU038370	Physa(Aplexa)	marmorata	1	Physidae	Hygrophila	Panpulmonata	Heterobranchia
AY651190	Physa	fontinalis	1	Physidae	Hygrophila	Panpulmonata	Heterobranchia
AY651189	Physa	fontinalis	1	Physidae	Hygrophila	Panpulmonata	Heterobranchia
AY651205	Physa	spelunca	1	Physidae	Hygrophila	Panpulmonata	Heterobranchia
AY651204	Physa	spelunca	1	Physidae	Hygrophila	Panpulmonata	Heterobranchia
KY012240.1	Ancylus	sp	2	Ancylidae	Hygrophila	Panpulmonata	Heterobranchia
MF545170.1	Ferrissia	rivularis	2	Ancylidae	Hygrophila	Panpulmonata	Heterobranchia
MF983606.1	Ferrissia	fragilis	2	Ancylidae	Hygrophila	Panpulmonata	Heterobranchia
KY849374.1	Ferrissia	california	2	Ancylidae	Hygrophila	Panpulmonata	Heterobranchia
EU038397	Gyraulus	parvus	2	Planorbidae	Hygrophila	Panpulmonata	Heterobranchia
EU038390	Glyptophysa	sp	2	Planorbidae	Hygrophila	Panpulmonata	Heterobranchia
EF012179	Glyptophysa	sp	2	Planorbidae	Hygrophila	Panpulmonata	Heterobranchia
AY651207	Biomphalaria	obstructa	2	Planorbidae	Hygrophila	Panpulmonata	Heterobranchia
EF012167	Biomphalaria	glabrata	2	Planorbidae	Hygrophila	Panpulmonata	Heterobranchia
NC_005439	Biomphalaria	glabrata	2	Planorbidae	Hygrophila	Panpulmonata	Heterobranchia
KY697249.1	Biomphalaria	straminea	2	Planorbidae	Hygrophila	Panpulmonata	Heterobranchia
MK279703.1	Biomphalaria	peregrina	2	Planorbidae	Hygrophila	Panpulmonata	Heterobranchia
MH593503.1	Biomphalaria	tenagophila	2	Planorbidae	Hygrophila	Panpulmonata	Heterobranchia
MH593417.1	Biomphalaria	occidentalis	2	Planorbidae	Hygrophila	Panpulmonata	Heterobranchia
MH593413.1	Biomphalaria	oligoza	2	Planorbidae	Hygrophila	Panpulmonata	Heterobranchia
MH593409.1	Biomphalaria	schrammi	2	Planorbidae	Hygrophila	Panpulmonata	Heterobranchia
MG780210.1	Biomphalaria	pfeifferi	2	Planorbidae	Hygrophila	Panpulmonata	Heterobranchia
KF926179.1	Biomphalaria	intermedia	2	Planorbidae	Hygrophila	Panpulmonata	Heterobranchia
DQ084843.1	Biomphalaria	sudanica	2	Planorbidae	Hygrophila	Panpulmonata	Heterobranchia
DQ084837.1	Biomphalaria	stanleyi	2	Planorbidae	Hygrophila	Panpulmonata	Heterobranchia
DQ084836.1	Biomphalaria	smithi	2	Planorbidae	Hygrophila	Panpulmonata	Heterobranchia
DQ084828.1	Biomphalaria	choanomphala	2	Planorbidae	Hygrophila	Panpulmonata	Heterobranchia
JX567601.1	Biomphalaria	crequii	2	Planorbidae	Hygrophila	Panpulmonata	Heterobranchia
JX567521.1	Biomphalaria	costata	2	Planorbidae	Hygrophila	Panpulmonata	Heterobranchia
EF012168	Choanomphalus	mackii	2	Planorbidae	Hygrophila	Panpulmonata	Heterobranchia
EF012166	Bathyomphalus	contortus	2	Planorbidae	Hygrophila	Panpulmonata	Heterobranchia
EF012165	Anisus	spirorbis	2	Planorbidae	Hygrophila	Panpulmonata	Heterobranchia
EF012173	Menetus	dilatatus	2	Planorbidae	Hygrophila	Panpulmonata	Heterobranchia
EF012170	Hippeutis	complanatus	2	Planorbidae	Hygrophila	Panpulmonata	Heterobranchia
MF458795.1	Planorbarius	corneus	2	Planorbidae	Hygrophila	Panpulmonata	Heterobranchia
EF012175	Planorbis	planorbis	2	Planorbidae	Hygrophila	Panpulmonata	Heterobranchia
KM612167.1	Planorbella	trivolvis	2	Planorbidae	Hygrophila	Panpulmonata	Heterobranchia
KF958031.1	Planorbella	campanulata	2	Planorbidae	Hygrophila	Panpulmonata	Heterobranchia
KM612145.1	Planorbella	anceps	2	Planorbidae	Hygrophila	Panpulmonata	Heterobranchia
EF012174	Planorbella	tenue	2	Planorbidae	Hygrophila	Panpulmonata	Heterobranchia
EF012178	Segmentina	nitida	2	Planorbidae	Hygrophila	Panpulmonata	Heterobranchia
EF012177	Segmentina	hemisphaerula	2	Planorbidae	Hygrophila	Panpulmonata	Heterobranchia
AY282587	Indoplanorbis	exustus	2	Planorbidae	Hygrophila	Panpulmonata	Heterobranchia
KT365867	Bulinus	truncatus	2	Planorbidae	Hygrophila	Panpulmonata	Heterobranchia
MN551574.1	Bulinus	forskalii	2	Planorbidae	Hygrophila	Panpulmonata	Heterobranchia
MN551572.1	Bulinus	tropicus	2	Planorbidae	Hygrophila	Panpulmonata	Heterobranchia
HQ121592.1	Bulinus	globosus	2	Planorbidae	Hygrophila	Panpulmonata	Heterobranchia
KJ157491.1	Bulinus	umbilicatus	2	Planorbidae	Hygrophila	Panpulmonata	Heterobranchia
KJ157487.1	Bulinus	senegalensis	2	Planorbidae	Hygrophila	Panpulmonata	Heterobranchia
AM286318.2	Bulinus	wrighti	2	Planorbidae	Hygrophila	Panpulmonata	Heterobranchia

AM286304.2	Bulinus	cernicus	2	Planorbidae	Hygrophila	Panpulmonata	Heterobranchia
AM286302.2	Bulinus	nasutus	2	Planorbidae	Hygrophila	Panpulmonata	Heterobranchia
AM286296.2	Bulinus	africanus	2	Planorbidae	Hygrophila	Panpulmonata	Heterobranchia
LT671981.1	Bulinus	crystallinus	2	Planorbidae	Hygrophila	Panpulmonata	Heterobranchia
LT671977.1	Bulinus	canescens	2	Planorbidae	Hygrophila	Panpulmonata	Heterobranchia
LT671975.1	Bulinus	angolensis	2	Planorbidae	Hygrophila	Panpulmonata	Heterobranchia
MF544613.1	Radix	auricularia	2	Lymnaeidae	Hygrophila	Panpulmonata	Heterobranchia
NC_026538	Radix	auricularia	2	Lymnaeidae	Hygrophila	Panpulmonata	Heterobranchia
GU736200.1	Radix	balthica	2	Lymnaeidae	Hygrophila	Panpulmonata	Heterobranchia
NC_026539	Radix	balthica	2	Lymnaeidae	Hygrophila	Panpulmonata	Heterobranchia
KY574609.1	Radix	rubiginosa	2	Lymnaeidae	Hygrophila	Panpulmonata	Heterobranchia
KT867322.1	Radix	zazurnensis	2	Lymnaeidae	Hygrophila	Panpulmonata	Heterobranchia
MN737035.1	Radix	plicatula	2	Lymnaeidae	Hygrophila	Panpulmonata	Heterobranchia
MN718578.1	Radix	euphratica	2	Lymnaeidae	Hygrophila	Panpulmonata	Heterobranchia
KX056254.1	Radix	labiata	2	Lymnaeidae	Hygrophila	Panpulmonata	Heterobranchia
EU818834.1	Radix	relicta	2	Lymnaeidae	Hygrophila	Panpulmonata	Heterobranchia
KM612193.1	Lymnaea	stagnalis	2	Lymnaeidae	Hygrophila	Panpulmonata	Heterobranchia
JN051381.1	Lymnaea	diaphana	2	Lymnaeidae	Hygrophila	Panpulmonata	Heterobranchia
JN051373.1	Lymnaea	viator	2	Lymnaeidae	Hygrophila	Panpulmonata	Heterobranchia
FN182199.1	Lymnaea	humilis	2	Lymnaeidae	Hygrophila	Panpulmonata	Heterobranchia
KP830107.1	Lymnaea	tumrokensis	2	Lymnaeidae	Hygrophila	Panpulmonata	Heterobranchia
JN051372.1	Galba	truncatula	2	Lymnaeidae	Hygrophila	Panpulmonata	Heterobranchia
MN095423.1	Galba	cousini	2	Lymnaeidae	Hygrophila	Panpulmonata	Heterobranchia
KT781336.1	Galba	cubensis	2	Lymnaeidae	Hygrophila	Panpulmonata	Heterobranchia
MN601426.1	Galba	mweruensis	2	Lymnaeidae	Hygrophila	Panpulmonata	Heterobranchia
FN356741.1	Galba	neotropica	2	Lymnaeidae	Hygrophila	Panpulmonata	Heterobranchia
JN614398.1	Galba	viatrix	2	Lymnaeidae	Hygrophila	Panpulmonata	Heterobranchia
NC_018536	Galba	pervia	2	Lymnaeidae	Hygrophila	Panpulmonata	Heterobranchia
MH087513.1	Pseudosuccinea	columella	2	Lymnaeidae	Hygrophila	Panpulmonata	Heterobranchia
MN102103.1	Acroloxus	coloradensis	2	Acroloxidae	Hygrophila	Panpulmonata	Heterobranchia
JQ646085.1	Acroloxus	lacustris	2	Acroloxidae	Hygrophila	Panpulmonata	Heterobranchia
JQ646078.1	Acroloxus	egirdirensis	2	Acroloxidae	Hygrophila	Panpulmonata	Heterobranchia
KY092829.1	Acroloxus	tetensi	2	Acroloxidae	Hygrophila	Panpulmonata	Heterobranchia
KY092827.1	Acroloxus	macedonicus	2	Acroloxidae	Hygrophila	Panpulmonata	Heterobranchia
KY092775.1	Acroloxus	improvisus	2	Acroloxidae	Hygrophila	Panpulmonata	Heterobranchia
KR822544.1	Acroloxus	victori	2	Acroloxidae	Hygrophila	Panpulmonata	Heterobranchia
KR822543.1	Acroloxus	likharevi	2	Acroloxidae	Hygrophila	Panpulmonata	Heterobranchia
KR822537.1	Acroloxus	baicalensis	2	Acroloxidae	Hygrophila	Panpulmonata	Heterobranchia
KC347574.1	Chilina	sanjuanina	2	Chilinoidae	Hygrophila	Panpulmonata	Heterobranchia
KT807839.1	Chilina	megastoma	2	Chilinoidae	Hygrophila	Panpulmonata	Heterobranchia
KT807838.1	Chilina	iguazuensis	2	Chilinoidae	Hygrophila	Panpulmonata	Heterobranchia
KT807834.1	Chilina	fluminea	2	Chilinoidae	Hygrophila	Panpulmonata	Heterobranchia
KC347575.1	Chilina	mendozana	2	Chilinoidae	Hygrophila	Panpulmonata	Heterobranchia
KT820423.1	Chilina	rushii	2	Chilinoidae	Hygrophila	Panpulmonata	Heterobranchia
KT820421.1	Chilina	gallardoi	2	Chilinoidae	Hygrophila	Panpulmonata	Heterobranchia
KT820419.1	Chilina	nicolasi	2	Chilinoidae	Hygrophila	Panpulmonata	Heterobranchia
KT820418.1	Chilina	santiagoi	2	Chilinoidae	Hygrophila	Panpulmonata	Heterobranchia
KC143970.1	Gastrocopta	bannertonensis	3	Gastrocoptidae	Eupulmonata	Panpulmonata	Heterobranchia
MN186467	Succinea	manaosensis	3	Succineidae	Eupulmonata	Panpulmonata	Heterobranchia
MN175956	Tomigerus	corrugatus	3	Odontostomidae	Eupulmonata	Panpulmonata	Heterobranchia
MK680002	Coccoglypta	pinchoniana	3	Bradybaenidae	Eupulmonata	Panpulmonata	Heterobranchia
MK883429	Cornu	aspersum	3	Helicidae	Eupulmonata	Panpulmonata	Heterobranchia
NC_021747	Cornu	aspersum	3	Helicidae	Eupulmonata	Panpulmonata	Heterobranchia
NC_001816	Cepaea	nemoralis	3	Helicidae	Eupulmonata	Panpulmonata	Heterobranchia
JF514659	Gaeotis	nigrolineata	3	Amphibulimidae	Eupulmonata	Panpulmonata	Heterobranchia
JF514658	Plekocheilus	vickeyi	3	Orthalicidae	Eupulmonata	Panpulmonata	Heterobranchia
JF514645	Megalobulimus	parafragilior	3	Megalobulimidae	Eupulmonata	Panpulmonata	Heterobranchia
JF514644	Pilsbrylia	paradoxa	3	Bulimulidae	Eupulmonata	Panpulmonata	Heterobranchia
KY216019	Samoana	fragilis	3	Partulidae	Eupulmonata	Panpulmonata	Heterobranchia
KX577717	Xerotricha	conspurcata	3	Hygromiidae	Eupulmonata	Panpulmonata	Heterobranchia
KT715846	Phaedusa	angustocostata	3	Clausiliidae	Eupulmonata	Panpulmonata	Heterobranchia
NC_001761	Albinaria	caerulea	3	Clausiliidae	Eupulmonata	Panpulmonata	Heterobranchia
EF057387	Satsuma	largillierti	3	Panpulmonata	Eupulmonata	Panpulmonata	Heterobranchia
EF057379	Camaena	longsonensis	3	Camaenidae	Eupulmonata	Panpulmonata	Heterobranchia
KJ631336	Achatina	fulica	3	Achatinidae	Eupulmonata	Panpulmonata	Heterobranchia
NC_030190	Achatinella	mustelina	3	Achatinellidae	Eupulmonata	Panpulmonata	Heterobranchia
KM518620	Pupilla	turcmenica	3	Pupillidae	Eupulmonata	Panpulmonata	Heterobranchia
NC_026044	Pupilla	muscorum	3	Pupillidae	Eupulmonata	Panpulmonata	Heterobranchia
NC_026043	Gastrocopta	cristata	3	Pupillidae	Eupulmonata	Panpulmonata	Heterobranchia
HM240412	Paraboysidia	tarutao	3	Vertiginidae	Eupulmonata	Panpulmonata	Heterobranchia
JX475060	Trochulus	plebeius	3	Hygromiidae	Eupulmonata	Panpulmonata	Heterobranchia
KX756234	Lauria	cylindracea	3	Punctidae	Eupulmonata	Panpulmonata	Heterobranchia
NC_030723	Cernuella	virgata	3	Geomitridae	Eupulmonata	Panpulmonata	Heterobranchia

MH383003	Zospeum	amoenum	3	Ellobiidae	Eupulmonata	Panpulmonata	Heterobranchia
NC_016175	Ovatella	vulcani	3	Ellobiidae	Eupulmonata	Panpulmonata	Heterobranchia
NC_016193	Trimusculus	reticulatus	3	Trimusculidae	Eupulmonata	Panpulmonata	Heterobranchia
MF983575	Atopos	sp	3	Rathouisiidae	Eupulmonata	Panpulmonata	Heterobranchia
KC206184	Veronicella	cubensis	3	Veronicellidae	Eupulmonata	Panpulmonata	Heterobranchia
NC_016183	Rhopalocaulis	grandidieri	3	Veronicellidae	Eupulmonata	Panpulmonata	Heterobranchia
MK312167	Preonia	persiae	3	Onchidiidae	Eupulmonata	Panpulmonata	Heterobranchia
NC_012376	Onchidella	celtica	3	Onchidiidae	Eupulmonata	Panpulmonata	Heterobranchia
EF489388	Trimusculus	afra	3	Trimusculidae	Eupulmonata	Panpulmonata	Heterobranchia
EF489389	Otina	ovata	3	Otinidae	Eupulmonata	Panpulmonata	Heterobranchia
MG935268	Turbonilla	jeffreysii	3	Pyramidellidae	Pyramidelloidea	Panpulmonata	Heterobranchia
MG421167.1	Odostoma	tenuisculpta	3	Pyramidellidae	Pyramidelloidea	Panpulmonata	Heterobranchia
NC_012435	Pyramidella	dolabrata	3	Pyramidellidae	Pyramidelloidea	Panpulmonata	Heterobranchia
JQ228488	Salinator	fragilis	3	Amphibolidae	Amphiboloidea	Panpulmonata	Heterobranchia
NC_016185	Salinator	rhamphidia	3	Amphibolidae	Amphiboloidea	Panpulmonata	Heterobranchia
JQ228469	Maningrida	arnhemensis	3	Maningrididae	Amphiboloidea	Panpulmonata	Heterobranchia
HQ660002	Phallomedusa	solida	3	Phallomedusidae	Amphiboloidea	Panpulmonata	Heterobranchia
JQ228467	Glacidorbis	hedleyi	3	Glacidorbidae	Glacidorboidea	Panpulmonata	Heterobranchia
JF819819	Microhedyle	odhneri	3	Microhedylidae	Acochlidiacea	Panpulmonata	Heterobranchia
JF819818	Parhedyle	tyrtowii	3	Parhedylidae	Acochlidiacea	Panpulmonata	Heterobranchia
AB914678	Aiteng	mysticus	3	Aitengidae	Acochlidiacea	Panpulmonata	Heterobranchia
JF819772	Pseudunela	marteli	3	Pseudunelidae	Acochlidiacea	Panpulmonata	Heterobranchia
JF819763	Strubelia	wawrai	3	Acochlidiidae	Acochlidiacea	Panpulmonata	Heterobranchia
HQ168460	Paraganitus	ellynnae	3	Ganitidae	Acochlidiacea	Panpulmonata	Heterobranchia
KF317068	Cylindrobulla	beauii	3	Cylindrobullidae	Sacoglossa	Panpulmonata	Heterobranchia
KF317067	Oxynoe	azuropunctata	3	Oxynoeidae	Sacoglossa	Panpulmonata	Heterobranchia
KF317065	Volvatella	ventricosa	3	Volvatellidae	Sacoglossa	Panpulmonata	Heterobranchia
MK919681	Elysia	crispata	3	Plakobranchidae	Sacoglossa	Panpulmonata	Heterobranchia
NC_030537	Elysia	ornata	3	Plakobranchidae	Sacoglossa	Panpulmonata	Heterobranchia
KU905830	Ercolania	fuscata	3	Limapontiidae	Sacoglossa	Panpulmonata	Heterobranchia
MK764394	Bosellia	mimetica	3	Boselliidae	Sacoglossa	Panpulmonata	Heterobranchia
MH087181	Polybranchia	schmekelae	3	Caliphyllidae	Sacoglossa	Panpulmonata	Heterobranchia
KJ610068	Costasiella	formicaria	3	Costasiellidae	Sacoglossa	Panpulmonata	Heterobranchia
KM086410	Julia	zebra	3	Juliidae	Sacoglossa	Panpulmonata	Heterobranchia
KM086409	Hermaea	wrangeliae	3	Hermaeidae	Sacoglossa	Panpulmonata	Heterobranchia
KM086405	Gascoignella	jabae	3	Platyhedylidae	Sacoglossa	Panpulmonata	Heterobranchia
KF644338	Siphonaria	thersites	3	Siphonariidae	Siphonarioidea	Panpulmonata	Heterobranchia
NC_016188	Siphonaria	gigas	3	Siphonariidae	Siphonarioidea	Panpulmonata	Heterobranchia
NC_012383	Siphonaria	pectinata	3	Siphonariidae	Siphonarioidea	Panpulmonata	Heterobranchia
KY574013.1	Viviparus	viviparus	4	Viviparidae	Viviparoidea	Architaenioglossa	Caenogastropoda
MK756270.1	Pomacea	occulta	4	Ampullariidae	Ampullarioidea	Architaenioglossa	Caenogastropoda
KX120967.1	Cochlostoma	cretense	4	Cochlostomatidae	Cyclophoroidea	Architaenioglossa	Caenogastropoda
MN153346.1	Cyclophorus	takumisatoi	4	Cyclophoridae	Cyclophoroidea	Architaenioglossa	Caenogastropoda
MG421673.1	Crepidula	williamsi	4	Calyptraeidae	Calyptraeoidae	Littorinimorpha	Caenogastropoda
AF546070.1	Capulus	ungaricus	4	Capulidae	Capuloidea	Littorinimorpha	Caenogastropoda
JF693370.1	Cypraea	tigris	4	Cypraeidae	Cypraeoidea	Littorinimorpha	Caenogastropoda
AY161628.1	Phenacovolva	weaveri	4	Ovulidae	Cypraeoidea	Littorinimorpha	Caenogastropoda
MN389091.1	Ficus	ficus	4	Ficidae	Ficoidea	Littorinimorpha	Caenogastropoda
MG421238.1	Littorina	littorea	4	Littorinidae	Littorinoidea	Littorinimorpha	Caenogastropoda
JF693404.1	Natica	lineata	4	Naticidae	Naticoidea	Littorinimorpha	Caenogastropoda
KX343198.1	Atlanta	selvagensis	4	Atlantidae	Pterotracheoidea	Littorinimorpha	Caenogastropoda
MG652385.1	Alvania	mediolittoralis	4	Rissoidae	Rissooidea	Littorinimorpha	Caenogastropoda
JF693435.1	Strombus	vittatus	4	Strombidae	Stromboidea	Littorinimorpha	Caenogastropoda
JF693439.1	Tonna	galea	4	Tonnidae	Tonnoidea	Littorinimorpha	Caenogastropoda
AF120635.1	Truncatella	guerinii	4	Truncatellidae	Truncatelloidea	Littorinimorpha	Caenogastropoda
AB930487.1	Vanikoro	helicoidea	4	Vanikoridae	Vanikoroidea	Littorinimorpha	Caenogastropoda
MG935041.1	Trivia	arctica	4	Triviidae	NA	Littorinimorpha	Caenogastropoda
EU495076.1	Dendropoma	petraeum	4	Vermetidae	Vermetoidea	Littorinimorpha	Caenogastropoda
NC_014583	Ceraesignum	maximum	4	Vermetidae	Littorinimorpha	Littorinimorpha	Caenogastropoda
HQ401587.1	Xenophora	solarioides	4	Xenophoridae	NA	Littorinimorpha	Caenogastropoda
MG422656.1	Buccinum	undatum	4	Buccinidae	Buccinoidea	Neogastropoda	Caenogastropoda
MG786112.1	onus	textile	4	Conidae	Conoidea	Neogastropoda	Caenogastropoda
NC_008797	Conus	textile	4	Conidae	Conoidea	Neogastropoda	Caenogastropoda
GU575382.1	Murex	pecten	4	Muricidae	Muricoidea	Neogastropoda	Caenogastropoda
KX233348.1	Oliva	todosina	4	Olividae	Volutoidea	Neogastropoda	Caenogastropoda
KU496561.1	Vexillum	tusum	4	Costellariidae	Turbinelloidea	Neogastropoda	Caenogastropoda
KF643721.1	Admete	viridula	4	Cancellariidae	Cancellarioidea	Neogastropoda	Caenogastropoda
JF693354.1	Cerithidea	cingulata	4	Potamididae	Cerithioidea	Sorbeoconcha	Caenogastropoda
MG423090.1	Pleurocera	acuta	4	Pleuroceridae	Cerithioidea	Sorbeoconcha	Caenogastropoda
KF926606.1	Semisulcospira	libertina	4	Semisulcospiridae	Cerithioidea	Sorbeoconcha	Caenogastropoda
AB845822.1	Batillaria	multiformis	4	Batillariidae	Cerithioidea	Sorbeoconcha	Caenogastropoda
MK879376.1	Melanopsis	etrusca	4	Melanopsidae	Cerithioidea	Sorbeoconcha	Caenogastropoda
GQ868078.1	Zeacumuantus	subcarinatus	4	Cerithiidae	Cerithioidea	Sorbeoconcha	Caenogastropoda

KR084908.1	Aplysia	punctata	4	Aplysiidae	Aplysioidea	Euopisthobranchia	Heterobranchia
NC_005827	Aplysia	californica	4	Aplysiidae	Aplysioidea	Euopisthobranchia	Heterobranchia
AF156143.1	Akera	bullata	4	Akeridae	Akeroidea	Euopisthobranchia	Heterobranchia
DQ974656.1	Bulla	ampulla	4	Bullidae	Bulloidea	Euopisthobranchia	Heterobranchia
KY094309.1	Pleurobranchus	maculata	4	Pleurobranchidae	Pleurobranchoidea	Nudipleura	Heterobranchia
JX680587.1	Doris	kerguelenensis	4	Doridiidae	Eudoridoidea	Nudipleura	Heterobranchia
KF643928.1	Aeolidia	papillosa	4	Aeolidiidae	Aeolidioidea	Nudipleura	Heterobranchia
KY129047.1	Fiona	pinnata	4	Fionidae	Fionoidea	Nudipleura	Heterobranchia
MF776823.1	Glaucus	atlanticus	4	Glaucidae	Aeolidioidea	Nudipleura	Heterobranchia
MN485347.1	Lunella	smaragdus	4	Trochidae	Trochoidea	Trochida	Vetigastropoda
GQ475034.1	Lepetodrilus	ovalis	4	Lepetodriloidae	Lepetodriloidea	Lepetellida	Vetigastropoda
NC_005940	Haliotis	rubra	4	Haliotidae	Haliotoidea	Lepetellida	Vetigastropoda
KY581542.1	Peltospira	delicata	4	Peltospiridae	Neomphaloidea	NA	Neomphalina
MF688020.1	Neritina	violacea	4	Neritidae	Neritoidea	Cycloneritida	Neritimorpha
GU810158	Nerita	melanotragus	4	Neritidae	Neritoidea	Cycloneritida	Neritimorpha
MK505446.1	Georissa	similis	4	Hydrocenidae	Hydrocenoidea	Cycloneritida	Neritimorpha
AB102709.1	Neritilia	cavernicola	4	Neritiliidae	Helicinoidea	Cycloneritida	Neritimorpha
KU566797.1	Patella	vulgata	4	Patellidae	Patelloidea	NA	Patellogastropoda
MN539281.1	Cocculina	enigmadonta	4	Cocculinidae	Cocculinoidea	NA	Cocculiniformia

Accession	Genus	species	Family	Clade 2	Clade 1
DQ238599	Lottia	digitalis	Lottiidae	Lottioidea	Patellogastropoda
GU810158	Nerita	melanotragus	Neritidae	Neritoidea	Neritimorpha
HM174253	Dendropoma	maximum	Vermetidae	Vermetoidea	Caenogastropoda, Littorinimorpha
KX155574	Conus	textile	Conidae	Conoidea	Caenogastropoda, Neogastropoda
AY569552	Aplysia	californica	Aplysiidae	Aplysioidea	Heterobranchia, Euthyneura, Tectipleura
AY345049	Siphonaria	pectinata	Siphonariidae	Siphonarioidea	Heterobranchia, Euthyneura, Panpulmonata
JN627205	Siphonaria	gigas	Siphonariidae	Siphonarioidea	Heterobranchia, Euthyneura, Panpulmonata
KU365324	Elysia	ornata	Plakobranchidae	Sacoglossa	Heterobranchia, Euthyneura, Panpulmonata
JN620539	Salinator	rhamphidia	Amphibolidae	Amphiboloidea	Heterobranchia, Euthyneura, Panpulmonata
JN632509	Trimusculus	reticulatus	Trimusculidae	Ellobiida	Heterobranchia, Euthyneura, Panpulmonata
JN615139	Ovatella	vulcani	Ellobiidae	Ellobiida	Heterobranchia, Euthyneura, Panpulmonata
AY345048	Onchidella	celtica	Onchidiidae	Systellommatophora	Heterobranchia, Euthyneura, Panpulmonata
AY345054	Pyramidella	dolabrata	Pyramidellidae	Pyramidelloidea	Heterobranchia, Euthyneura, Panpulmonata
JN619347	Rhopalocaulis	grandidieri	Veronicellidae	Systellommatophora	Heterobranchia, Euthyneura, Panpulmonata
KR736333	Cernuella	virgata	Geomitridae	Eupulmonata, Stylommatophora	Heterobranchia, Euthyneura, Panpulmonata
JQ417194	Helix	aspersa	Helicidae	Eupulmonata, Stylommatophora	Heterobranchia, Euthyneura, Panpulmonata
U23045	Cepaea	nemoralis	Helicidae	Eupulmonata, Stylommatophora	Heterobranchia, Euthyneura, Panpulmonata
X83390	Albinaria	caerulea	Clausiliidae	Eupulmonata, Stylommatophora	Heterobranchia, Euthyneura, Panpulmonata
KU525108	Achatinella	mustelina	Achatinellidae	Eupulmonata, Stylommatophora	Heterobranchia, Euthyneura, Panpulmonata
KC185404	Pupilla	muscorum	Pupillidae	Eupulmonata, Stylommatophora	Heterobranchia, Euthyneura, Panpulmonata
KC185403	Gastrocopta	cristata	Pupillidae	Eupulmonata, Stylommatophora	Heterobranchia, Euthyneura, Panpulmonata
KP098541	Radix	balthica	Lymnaeidae	Hygrophila	Heterobranchia, Euthyneura, Panpulmonata
KP098540	Radix	auricularia	Lymnaeidae	Hygrophila	Heterobranchia, Euthyneura, Panpulmonata
JN564796	Galba	pervia	Lymnaeidae	Hygrophila	Heterobranchia, Euthyneura, Panpulmonata
MT862415	Planorbarius	corneus	Planorbidae	Hygrophila	Heterobranchia, Euthyneura, Panpulmonata
AY380567	Biomphalaria	glabrata	Planorbidae	Hygrophila	Heterobranchia, Euthyneura, Panpulmonata
SRX565294	Physa	gyrina	Physidae	Hygrophila	Heterobranchia, Euthyneura, Panpulmonata
JQ390525	Physa	acuta (isolate A)	Physidae	Hygrophila	Heterobranchia, Euthyneura, Panpulmonata
JQ390526	Physa	acuta (isolate B)	Physidae	Hygrophila	Heterobranchia, Euthyneura, Panpulmonata

Supplementary data S1C

Accession COI	Accession 16S	Taxon (1)	Taxon (2)	Isolate
EU038367	EU038320	Physa acuta N	Physella acuta	CUB3
EU038366	EU038319	Physa acuta N	Physella acuta	CUB2
EU038365	EU038318	Physa acuta N	Physella acuta	CUB1
EU038361	EU038314	Physa acuta N	Physella acuta	CARR2
EU038356	EU038309	Physa acuta N	Physella acuta	CAnr1
EU038368	EU038321	Physa acuta N	Physella acuta	F13
EU038355	EU038308	Physa acuta N	Physella acuta	argrv3
EU038372	EU038325	Physa acuta N	Physella acuta	inN19
EU038371	EU038324	Physa acuta N	Physella acuta	inN1
EU038389	EU038342	Physa acuta N	Physella acuta	NNA2
AY651170	AY651209	Physa acuta N	Physella virgata	argrv1
AY65117	AY651210	Physa acuta N	Physella virgata	argrv2
AY651174	AY651213	Physa acuta N	Physa acuta	co42241
AY651175	AY651214	Physa acuta N	Physella anatina	co43888
AY651176	AY651215	Physa acuta N	Physella anatina	co43906
AY651177	AY651216	Physa acuta N	Physella anatina	co43914
AY651181	AY651219	Physa acuta N	Physa acuta	coa021
AY651183	AY651221	Physa acuta N	Physella cupreonitens	coCUP1
AY651184	AY651222	Physa acuta N	Physella cupreonitens	coCUP2
AY651185	AY651223	Physa acuta N	Physa acuta	F23
AY651186	AY651224	Physa acuta N	Physa acuta	F7
AY651188	AY651226	Physa acuta N	Physa acuta	mo40408
AY651192	AY651230	Physa acuta N	Physa heterostropha	paP10
AY651193	AY651231	Physa acuta N	Physa heterostropha	paP9
AY651203	AY651241	Physa acuta N	Physa acuta	wybhr2
GQ415033	GQ415012	Physa acuta N	Physa acuta	C2
GQ415034	GQ415013	Physa acuta N	Physa acuta	C3
GQ415035	GQ415014	Physa acuta N	Physa acuta	C5
GQ415037	GQ415015	Physa acuta N	Physa acuta	C11
GQ415039	GQ415016	Physa acuta N	Physa acuta	C14
AY651204	AY651242	Physa acuta N	Physella spelunca	wySPE1
AY651205	AY651243	Physa acuta N	Physella spelunca	wySPE2
EU038395	EU038348	Physa carolinae	Physa sp. scjni1	scjni1
EU038396	EU038349	Physa carolinae	Physa sp. Scjni2	scjni2
GQ415040	GQ415022	Physa carolinae	Physa sp. ARW-2009	blac1
GQ415041	GQ415024	Physa carolinae	Physa sp. ARW-2009	bull1
GQ415042	GQ415025	Physa carolinae	Physa sp. ARW-2009	bull2
GQ415043	GQ415026	Physa carolinae	Physa sp. ARW-2009	hell1
AY651198	AY651236	Physa zionis	Petrophysa zionis	utznp1
AY651194	AY651232	Physa pomilia	Physella hendersoni	scysr1
AY651195	AY651233	Physa pomilia	Physella hendersoni	scysr2
AY651196	AY651234	Physa pomilia	Physella hendersoni	scysr3

EU038353	EU038306	Physa pomilia	Physa pomilia	alpom1
EU038354	EU038307	Physa pomilia	Physa pomilia	alpom2
EU038363	EU038316	Physa pomilia	Physa pomilia	ctbbsp1
EU038364	EU038317	Physa pomilia	Physa pomilia	ctbbsp5
AF346740	AF346752	Physa gyrina	Physella gyrina	PgyCB
AF346741	AF346753	Physa gyrina	Physella gyrina	PgyML
AF346742	AF346754	Physa gyrina	Physella gyrina	PgyFM
AF346743	AF346755	Physa gyrina	Physella gyrina	PgyCL
AF346744	AF346756	Physa gyrina	Physella gyrina	PgyFLY
AF346745	AF346757	Physa gyrina	Physella wrighti	---
AF346735	AF346747	Physa gyrina	Physella johnsoni	PjoMI
AF346736	AF346748	Physa gyrina	Physella johnsoni	PjoLO
AF346737	AF346749	Physa gyrina	Physella johnsoni	PjoBA
AF346738	AF346750	Physa gyrina	Physella johnsoni	PjoUP
AF346739	AF346751	Physa gyrina	Physella johnsoni	PloCAC
AY651201	AY651239	Physa gyrina	Physella aurea	vajsv1
AY651202	AY651240	Physa gyrina	Physella aurea	vahsv2
AY651197	AY651235	Physa gyrina	Physella gyrina	ut37088
AY651199	AY651237	Physa gyrina	Physella gyrina	vascg1
AY651200	AY651238	Physa gyrina	Physella gyrina	vascg2
AY651191	AY651229	Physa gyrina	Physella gyrina	ok42234
AY651187	AY651229	Physa gyrina	Physella gyrina	iobrg1
AY651172	AY651211	Physa gyrina	Physella johnsoni	CApjon1
AY651173	AY651212	Physa gyrina	Physella johnsoni	CApjon2
AY651178	AY651217	Physa gyrina	Physella gyrina	co43936
AY651180	AY651218	Physa gyrina	Physella gyrina	coa007
AY651182	AY651220	Physa gyrina	Physella gyrina	coa030
EU038398	EU038351	Physa gyrina	Physella gyrina	utfl2
EU038374	EU038327	Physa gyrina	Physella gyrina	kiKSC2
EU038373	EU038326	Physa gyrina	Physella gyrina	kyksc1
EU038358	EU038311	Physa ancillaria	Physella ancillaria	CAOR1
EU038359	EU038312	Physa ancillaria	Physella ancillaria	CAor2
EU038378	EU038331	Physa ancillaria	Physella ancillaria	miclm3
EU038379	EU038332	Physa ancillaria	Physella ancillaria	miclm4
EU038380	EU038333	Physa ancillaria	Physella ancillaria	midlp1
EU038381	U038334	Physa ancillaria	Physella ancillaria	midlp2
EU038382	EU038335	Physa ancillaria	Physella ancillaria	midlp3
EU038383	EU038336	Physa ancillaria	Physella ancillaria	miFKP1
EU038384	EU038337	Physa ancillaria	Physella ancillaria	miFKP2
EU038385	EU038338	Physa ancillaria	Physella ancillaria	mihgp1
EU038387	EU038340	Physa ancillaria	Physella ancillaria	miptg1
EU038388	EU038341	Physa ancillaria	Physella ancillaria	miPTG2
EU038391	EU038344	Physa ancillaria	Physella ancillaria	paDWR3
EU038392	EU038345	Physa ancillaria	Physella ancillaria	padr1
AF346746	AF346758	Physa jennessi	Physa sp. RLHL-2001	---
FJ373018	AY651227	Physa fontinalis	Physa fontinalis	---
AY651190	AY651228	Physa fontinalis	Physa fontinalis	Nnf1
AY577505	AY577465	Physa fontinalis	Physa fontinalis	Nnf2
EU038375	EU038328	Physa vernalis	Physa vernalis	maamb1
EU038376	EU038329	Physa vernalis	Physa vernalis	maamb2

EU038369	EU038322	Physa marmorata	Physa marmorata	Gmar1
EU038370	EU038323	Physa marmorata	Physa marmorata	Gmar2
EU038377	U038330	Aplexa elongata	Aplexa elongata	miall1
EU038352	EU038305	LYMNAEIDAE	Ladislavella elodes	44106
EU038362	EU038315	LYMNAEIDAE	Fossaria bulimoides	co42263
AY651206	AY651244	LYMNAEIDAE	Pseudosuccinea columella	mi4mpc1
AY651207	AY651245	ANCYLOPLANORBIDAE	Biomphalaria obstructa	scBCTL1
AY651208	AY651241	ANCYLOPLANORBIDAE	Planorbella trivolvis	16PB2h
EU038397	EU038350	ANCYLOPLANORBIDAE	Planorbella trivolvis	scPC3
EU038393	EU038346	ANCYLOPLANORBIDAE	Laevapex fuscus	scAB1
EU038394	EU038347	ANCYLOPLANORBIDAE	Gyraulus parvus	scgtvs3
EU038390	EU038343	ANCYLOPLANORBIDAE	Glyptophysa sp.	NZla2

focal snails	pairing session	focal status	partner	trait	Nb of pairs	mean ± SE or successes / failures		test of type effect (1df)	Random effects included	model type
						Type N	Type D			
G1-1	1	virgin	virgin albino	nb of male attempts	103	1.21 ± 0.11	0.50 ± 0.11	**χ^2=14.63, *P*= 1.3 10^{-4}**	matriline, ind	Poisson
G1-1	1	virgin	virgin albino	male copulation (yes/no)	103	36 / 17	11 / 39	**χ^2=13.26, *P*= 2.7 10^{-4}**	matriline, ind	Binomial
G1-1	1	virgin	virgin albino	male time	103	0.22 ± 0.03	0.06 ± 0.02	**χ^2=15.02, *P*= 1.0 10^{-4}**	matriline	Gaussian
G1-1	1	virgin	virgin albino	nb of female attempts	103	1.53 ± 0.11	1.48 ± 0.11	χ^2=0.04, *P*= 0.84	matriline, ind	Poisson
G1-1	1	virgin	virgin albino	female copulation (yes/no)	103	47 / 6	44 / 6	χ^2=0.18, *P*= 0.67	matriline, ind	Binomial
G1-1	1	virgin	virgin albino	female time	103	0.24 ± 0.02	0.27 ± 0.02	χ^2=1.58, *P*= 0.21	matriline	Gaussian
G1-2	2	experienced	experienced albino	nb of male attempts	74	0.98 ± 0.10	0.25 ± 0.10	**χ^2=16.02, *P*= 6.3 10^{-5}**	matriline, ind	Poisson
G1-2	2	experienced	experienced albino	male copulation (yes/no)	74	27 / 15	4 / 28	**χ^2=18.04, *P*= 2.2 10^{-5}**	matriline, ind	Binomial
G1-2	2	experienced	experienced albino	male time	74	0.22 ± 0.03	0.03 ± 0.01	**χ^2=23.7, *P*= 1.1 10^{-6}**	matriline	Gaussian
G1-2	2	experienced	experienced albino	nb of female attempts	74	1.20 ± 0.10	1.06 ± 0.15	χ^2=0.26, *P*= 0.61	matriline, ind	Poisson
G1-2	2	experienced	experienced albino	female copulation (yes/no)	74	32 / 10	25 / 7	χ^2=0.05, *P*= 0.83	matriline, ind	Binomial
G1-2	2	experienced	experienced albino	female time	74	0.26 ± 0.03	0.26 ± 0.04	χ^2=0.01, *P*= 0.93	matriline	Gaussian

focal snails	pairing session	status	trait	Nb of pairs	mean ± SE or successes / failures				test of type effect (1df)	test of partner type effect (1df)	interaction	Random effects included	model type
					N with N	D with N	N with D	D with D					
G1-2	1	virgin	nb of male attempts	37	1.33 ± 0.16	0.38 ± 0.14	0.89 ± 0.15	0.22 ± 0.20	**χ^2=16.1, *P*= 6.0 10^{-5}**	χ^2=2.56, *P*= 0.11	χ^2=0.06, *P* =0.80	matriline, pair, ind	Poisson
G1-2	1	virgin	male copulation (yes/no)	37	17 / 7	4 / 14	12 / 6	2 / 12	**χ^2=16.4, *P*= 5.2 10^{-5}**	χ^2=0.33, *P*= 0.57	χ^2=0.09, *P* =0.77	matriline, pair, ind	Binomial
G1-2	1	virgin	male time	37	0.299 ± 0.044	0.074 ± 0.042	0.190 ± 0.047	0.057 ± 0.046	**χ^2=10.39, *P*= 0.0013 (0.002)[2]**	χ^2=3.52, *P*= 0.061 (0.041)[2]	χ^2=1.64, *P* =0.20 (0.218)[2]	matriline, pair	Gaussian
G1-1	3	experienced	nb of male attempts	49	0.79 ± 0.15	0.08 ± 0.07	0.80 ± 0.14	0.07 ± 0.07	**χ^2=24.83, *P*= 6.3 10^{-7}**	χ^2=0.01, *P*= 0.92	χ^2=0.02, *P* =0.89	matriline, pair, ind	Poisson
G1-1	3	experienced	male copulation (yes/no)	49	7 / 17	1 / 25	13 / 13	1 / 21	**χ^2=20.1, *P*= 6.3 10^{-6}**	χ^2=2.09, *P*= 0.15	χ^2=0.21, *P* =0.64	none[1]	Binomial
G1-1	3	experienced	male time	49	0.087 ± 0.062	0.025 ± 0.020	0.255 ± 0.048	0.011 ± 0.022	**(partner N) χ^2=5.70, *P*= 0.017 (0.036)[2]**	**(focal N) χ^2=5.24, *P*= 0.022 (0.003)[2]**	**χ^2=7.01, *P* =0.008 (0.003)[2]**	matriline, pair	Gaussian
									(partner D) χ^2=7.75, *P*= 0.005 (<0.001)[2]	(focal D) χ^2=0.34, *P*= 0.56 (0.67)[2]			

[1] model is not overdispersed, and diverges when including random effects. A conservative test, robust to potential within-pair correlations, was made by keeping only one individual per pair; the results were the same (interaction χ^2=0.15, P=0.69; type effect χ^2=8.44, P=0.004; partner type χ^2=0.93, P=0.33)

[2] in brackets, two-tailed p-values from nonparametric tests using permutations (random reattribution of mitotypes among families)

focal snails	pairing session	status	partner	trait	N	mean ± SE or successes/failures		test of type effect (1df)	Random effects	model type
						Type N	Type D			
G1-1	1	virgin	virgin albino	eggs laid by mate	103	59.37 ± 2.95 (52/1)	17.46 ± 5.11 (19/31)	**χ^2=28.3, *P*= 1.0 10^{-7} (<10^{-4})[4]**	matriline	Gaussian
G1-1	1	virgin	virgin albino	paternity share	71	0.94 ± 0.03 (50/2)	0.11 ± 0.11 (4/15)	**χ^2=57.7, *P*= 3.1 10^{-14}**	matriline, ind	Binomial
G1-1	1	virgin	virgin albino	male fitness	103	44.85 ± 2.35 (50/3)	3.08 ± 3.07 (4/46)	**χ^2=42.2, *P*= 8.3 10^{-11} (<10^{-4})[4]**	matriline	Gaussian
G1-1	1	virgin	virgin albino	eggs laid	103	42.76 ± 3.26	47.36 ± 3.50	χ^2=0.93, *P*= 0.33	matriline	Gaussian
G1-1	1	virgin	virgin albino	egg survival	99	0.74 ± 0.03	0.73 ± 0.05	χ^2=0.02, *P*= 0.90	matriline, ind	Binomial
G1-1	1	virgin	virgin albino	female fitness[3]	103	31.77 ± 2.85	34.81 ± 2.96	χ^2=0.57, *P*= 0.45	matriline	Gaussian
G1-1	2	experienced	nonvirgin albino	eggs laid by mate	100	49.00 ± 2.72	50.94 ± 3.713	χ^2=0.17, *P*= 0.68	matriline	Gaussian
G1-1	2	experienced	nonvirgin albino	paternity share	98	0.41 ± 0.05 (38/11)	0.025 ± 0.02 (2/47)	**χ^2=33.2, *P*= 8.1 10^{-9}**	matriline, ind	Binomial
G1-1	2	experienced	nonvirgin albino	male fitness[3]	100	13.95 ± 2.44 (38/13)	0.65 ± 0.53 (2/47)	**χ^2=18.6, *P*= 1.6 10^{-5} (10^{-4})[4]**	matriline	Gaussian

[3] female fitness is the number of juveniles (hatched and alive at 14 days) obtained from eggs laid by the focal individual in three days
male fitness is the number of juveniles sired by the focal, obtained from eggs laid by the focal's partner in three days

[4] in brackets, two-tailed p-values from nonparametric test using permutations (random reattribution of mitotypes among families, keeping pairs unchanged)

focal snails	pairing session	trait	Nb of inds	means ± SE and successes / failures				test of type effect (1df)	test of partner type effect (1 df)	Interaction (1 df)	Random effects	model type
				N with N[(5)]	D with N[(5)]	N with D[(5)]	D with D[(5)]					
G1-2	1	eggs laid	74	46.50 ± 4.54 (23 / 1)	50.93 ± 7.58 (17 / 1)	8.78 ± 4.05 (7 / 11)	5.14 ± 4.99 (2 / 12)	χ^2=0.02, *P*= 0.89 (0.92)	**χ^2=49.34, *P*= 2.1 10^{-12} (0.0002)**	χ^2=0.89, P=0.35 (0.55)	matriline	Poisson
G1-2	1	egg survival	49	0.59 ± 0.06	0.76 ± 0.06	0.57 ± 0.13	0.43 ± 0.43	χ^2=2.21, *P*= 0.14	χ^2=3.24, P=0.07	χ^2=0.07, P=0.79	matriline, ind	Binomial
G1-2	1	female fitness	73	28.75 ± 4.07 (21 / 3)	39.36 ± 5.53 (17 / 1)	5.50 ± 2.64 (6 / 12)	4.29 ± 4.29 (1 / 13)	χ^2=1.52, *P*= 0.22 (0.29)	**χ^2=35.4, *P*= 2.66 10^{-9} (0.0001)**	χ^2=2.03, P=0.15 (0.24)	matriline	Gaussian

[(5)] In « N with N », « D with N » etc., the first individual is the focal (on which traits are measured), the second is the partner

focal snails	pairing session	status	partner	trait	N	mean ± SE or successes/failures		test of type effect (1df)	Random effects	model type
						Type N	Type D			
G2-1	none	none	none	laid clutches or died (1/0)	256	121 / 13	74 / 48	χ^2=18.7, *P*= 1.5 10^{-5}	matriline [6]	Binomial
G2-1	none	none	none	age at egg-laying (days)	195	69.40 ± 1.55	87.88 ± 2.90	χ^2=22.1, *P*= 2.6 10^{-6}	matriline	Gaussian
G2-1	none	none	none	self-fertilization fitness[8]	256	20.11 ± 3.29 (96/38)	1.23 ± 0.52 (14/108)	χ^2=18.7, *P*= 1.5 10^{-5} (<10^{-4})[7]	matriline	Gaussian

[6] individual was not added as a random factor as it made the model diverge, and there was no overdispersion

[7] in brackets, two-tailed p-values from nonparametric test using permutations (random reattribution of mitotypes among families)

[8] self-fertilization fitness is the number of live offspring produced by the isolated snail during the experiment

trait	Nb of individuals	Body weight (mg) effect		Mitotype effect			random terms	Distribution
		coefficient	test	N mean	D mean	test		
Seminal vesicle size (mm^2)	42	0.011+/- 0.006	X^2=3.63, *P*= 0.057	3.44 +/- 0.26	1.40 +/- 0.15	**X^2=30.04, *P*= 4.22.10^{-8}**	matriline	Gaussian
Sperm count (x1000)	63	0.020+/- 0.008	**X^2=5.63, *P*= 0.018**	168.6 +/- 27.3	4.83 +/- 3.03	**X^2=38.55, *P*= 5.32.10^{-10}**	matriline, ind, observation	Poisson